Liu, C., Ueno, T., Kuse, S., Saito, F., Nitta, T., Piali, L., Nakano, H., Kakiuchi, T., Lipp, M., Hollander, G.A., and Takahama, Y. (2005). The role of CCL21 in recruitment of T-precursor cells to fetal thymi. Blood *105*, 31–39.

Matloubian, M., Lo, C.G., Cinamon, G., Lesneski, M.J., Xu, Y., Brinkmann, V., Allende, M.L., Proia, R.L., and Cyster, J.G. (2004). Lymphocyte egress from thymus and peripheral lymphoid organs is dependent on S1P receptor 1. Nature *427*, 355–360.

Miller, J.F.A.P. (1961). Immunological function of the thymus. Lancet *2*, 748–749.

Misslitz, A., Pabst, O., Hintzen, G., Ohl, L., Kremmer, E., Petrie, H.T., and Forster, R. (2004). Thymic T cell development and progenitor localization depend on CCR7. J. Exp. Med. *200*, 481–491.

Moore, N.C., Anderson, G., McLoughlin, D.E., Owen, J.J., and Jenkinson, E.J. (1994). Differential expression of Mtv loci in MHC class II-positive thymic stromal cells. J. Immunol. *152*, 4826–4831.

Nagamine, K., Peterson, P., Scott, H.S., Kudoh, J., Minoshima, S., Heino, M., Krohn, K.J., Lalioti, M.D., Mullis, P.E., Antonarakis, S.E., et al. (1997). Positional cloning of the APECED gene. Nat. Genet. *17*, 393–398.

Nakano, H., Mori, S., Yonekawa, H., Nariuchi, H., Matsuzawa, A., and Kakiuchi, T. (1998). A novel mutant gene involved in T-lymphocyte-specific homing into peripheral lymphoid organs on mouse chromosome 4. Blood *91*, 2886–2895.

Palmer, E. (2003). Negative selection—clearing out the bad apples from the T-cell repertoire. Nat. Rev. Immunol. *3*, 383–391.

Plotkin, J., Prockop, S.E., Lepique, A., and Petrie, H.T. (2003). Critical role for CXCR4 signaling in progenitor localization and T cell differentiation in the postnatal thymus. J. Immunol. *171*, 4521–4527.

Ramsdell, F., Jenkins, M., Dinh, Q., and Fowlkes, B.J. (1991). The majority of CD4+8-thymocytes are functionally immature. J. Immunol. *147*, 1779–1785.

Reichert, R.A., Gallatin, W.M., Butcher, E.C., and Weissman, I.L. (1984). A homing receptor-bearing cortical thymocyte subset: implications for thymus cell migration and the nature of cortisone-resistant thymocytes. Cell *38*, 89–99.

Reichert, R.A., Weissman, I.L., and Butcher, E.C. (1986a). Phenotypic analysis of thymocytes that express homing receptors for peripheral lymph nodes. J. Immunol. *136*, 3521–3528.

Reichert, R.A., Jerabek, L., Gallatin, W.M., Butcher, E.C., and Weissman, I.L. (1986b). Ontogeny of lymphocyte homing receptor expression in the mouse thymus. J. Immunol. *136*, 3535–3542.

Rinderle, C., Christensen, H.M., Schweiger, S., Lehrach, H., and Yaspo, M.L. (1999). AIRE encodes a nuclear protein co-localizing with cytoskeletal filaments: altered sub-cellular distribution of mutants lacking the PHD zinc fingers. Hum. Mol. Genet. *8*, 277–290.

Ritter, M.A., and Boyd, R.L. (1993). Development in the thymus: it takes two to tango. Immunol. Today *14*, 462–469.

Scollay, R., and Godfrey, D.I. (1995). Thymic emigration: conveyor belts or lucky dips? Immunol. Today *16*, 268–274.

Sheard, M.A., Liu, C., and Takahama, Y. (2004). Developmental status of CD4–CD8$^+$ and CD4+CD8$^-$ thymocytes with medium expression of CD3. Eur. J. Immunol. *34*, 25–35.

Shinkai, Y., Koyasu, S., Nakayama, K., Murphy, K.M., Loh, D.Y., Reinherz, E.L., and Alt, F.W. (1993). Restoration of T cell development in RAG-2-deficient mice by functional TCR transgenes. Science *259*, 822–825.

Takahama, Y., Letterio, J.J., Suzuki, H., Farr, A.G., and Singer, A. (1994). Early progression of thymocytes along the CD4/CD8 developmental pathway is regulated by a subset of thymic epithelial cells expressing transforming growth factor beta. J. Exp. Med. *179*, 1495–1506.

Ueno, T., Hara, K., Willis, M.S., Malin, M.A., Hopken, U.E., Gray, D.H., Matsushima, K., Lipp, M., Springer, T.A., Boyd, R.L., et al. (2002). Role for CCR7 ligands in the emigration of newly generated T lymphocytes from the neonatal thymus. Immunity *16*, 205–218.

Ueno, T., Saito, F., Gray, D.H., Kuse, S., Hieshima, K., Nakano, H., Kakiuchi, T., Lipp, M., Boyd, R.L., and Takahama, Y. (2004). CCR7 signals are essential for cortex-to-medulla migration of developing thymocytes. J. Exp. Med. *200*, 493–505.

Ushiki, T. (1986). A scanning electron-microscopic study of the rat thymus with special reference to cell types and migration of lymphocytes into the general circulation. Cell Tissue Res. *244*, 285–298.

van Ewijk, W., Shores, E.W., and Singer, A. (1994). Crosstalk in the mouse thymus. Immunol. Today *15*, 214–217.

van Vliet, E., Melis, M., and van Ewijk, W. (1984). Immunohistology of thymic nurse cells. Cell. Immunol. *87*, 101–109.

White, S.C., and Casarett, G.W. (1974). Induction of experimental autoallergic sialadenitis. J. Immunol. *112*, 178–185.

Witt, C.M., Raychaudhuri, S., Schaefer, B., Chakraborty, A.K., and Robey, E.A. (2005). Directed migration of positively selected thymocytes visualized in real time. PLoS Biol. *3* (6), e160 DOI: 10.1371/journal.pbio.0030160.

Zuklys, S., Balciunaite, G., Agarwal, A., Fasler-Kan, E., Palmer, E., and Hollander, G.A. (2000). Normal thymic architecture and negative selection are associated with Aire expression, the gene defective in the autoimmune-polyendocrinopathy-candidiasis-ectodermal dystrophy (APECED). J. Immunol. *165*, 1976–1983.

FEBS Letters 580 (2006) 3699–3705

A novel apoptosis cascade mediated by lysosomal lactoferrin and its participation in hepatocyte apoptosis induced by D-galactosamine

Nobuhiko Katunuma[a,*], Quang Trong Le[a], Etsuko Murata[a], Atsushi Matsui[a], Eiji Majima[b], Naozumi Ishimaru[c], Yoshio Hayashi[c], Atsushi Ohashi[a]

[a] *Institute for Health Sciences, Tokushima Bunri University, 180 Nishihamabouji, Yamashiro-cho, Tokushima 770-8514, Japan*
[b] *APRO Life Science Institute, 124-4 Itayashima, Myojin, Seto-cho, Naruto City, Tokushima 771-0360, Japan*
[c] *School of Dentistry, Tokushima University, 3-18-15 Kuramoto-cho, Tokushima 770-8504, Japan*

Received 12 April 2006; revised 25 May 2006; accepted 26 May 2006

Available online 5 June 2006

Edited by Vladimir Skulachev

Abstract **A new apoptosis cascade mediated by lysosomal lactoferrin was found in apoptotic liver induced by D-galactosamine. Caspase-3 and lactoferrin were increased in the apoptotic liver cytoplasm and serum transaminases were elevated. Recombinant lactoferrin stimulated procaspase-3 processing at 10^{-6}–10^{-7} M to an extent similar to that by granzyme B in vitro. Lactoferrin changed procaspase-3 structure susceptible to the processing. Synthetic peptide Y_{679}-K_{695} in lactoferrin molecule inhibited the processing of procaspase-3 by lactoferrin. Lactoferrin in lysosomes was decreased and lactoferrin released into cytoplasm was increased quantitatively in D-galactosamine induced apoptotic liver, and procaspase-3 in cytoplasm was processed to caspase-3.**

Keywords: Apoptosis; Procaspase-3; Lactoferrin; Processing; Lysosome; D-Galactosamine

1. Introduction

Many apoptosis cascades have been reported, and mitochondrial factor mediated apoptosis cascades have been well established. Caspase-3 plays a central role in various apoptosis cascades as an executive enzyme [1–4]. In 1998, we found that an unknown protein extracted from lysosomes by digitonin enhanced procaspase-3 processing in liver cytoplasm [5,6]. After that, we determined that the activating factor was lactoferrin and suggested preliminary the existence of a new apoptosis cascade mediated by lysosomal lactoferrin [7]. This paper reports on the stimulation mechanisms of procaspase-3 processing by lactoferrin at the enzymological aspects in detail and the releasing mechanism of lysosomal lactoferrin into cytoplasm in D-galactosamine-induced apoptotic hepatocyte. The pathological aspects of severe liver injury induced by D-galactosamine have been well characterized by TUNEL staining and also DNA fragmentation [9–11]. We reported in a previous paper that caspase-3 in the cytoplasm of apoptosis liver induced by D-galactosamine was increased and the apoptosis was protected by epigallo-catechin gallate in green tea which inhibited caspase-3 [11].

As the next step, we studied the molecular mechanism underlying increases in the activity of activated caspase-3 in the cytoplasm in vivo and found that a new procaspase-3 activating protein was released into the cytoplasm from lysosomes in D-galactosamine induced apoptotic hepatocytes. We determined that this activating protein was a lactoferrin originally located in lysosomes. Recombinant pure lactoferrin was found to strongly stimulate procaspase-3 processing to form active caspase-3 as same extent to that by granzyme B in vitro, and the activation mechanisms were studied at the molecular level. We reported that releasing mechanism of lysosomal lactoferrin into the cytoplasm in D-galactosamine induced apoptotic rat liver in vivo.

This paper reports on (1) stimulation mechanism of procaspase-3 processing by lactoferrin in vitro; (2) the mechanism by which lysosomal lactoferrin is released into the cytoplasm after D-galactosamine administration in vivo; (3) the existence of a novel apoptosis cascade mediated by lysosomal lactoferrin.

2. Materials and methods

2.1. Chemicals used

Caspase-3, procaspase-3, lipopolysaccharide (LPS), and lactoferrin were all recombinant pure proteins purchased from Sigma Co. (USA). The 17 residue peptide Y_{679}-K_{695} (YEKYLGPQYVAGITNLK) of the lactoferrin molecule was chemically synthesized by Asahi Techno-glass (Chiba, Japan) with 95% purity. Aspartylglutamylvalinylaspartyl-7-amino-4-trifluoromethylcoumarin (DEVD-AFC) was purchased from Peptide Institute Inc., Osaka, Japan.

2.2. Assay of procaspase-3 processing activity

Caspase-3 activity derived from procaspase-3 was determined from the fluorescence of AFC released from DEVD-AFC [5,11], and the enzyme activity was expressed in terms of AFC released in nmol/h/μg protein or nmol/h [5,6,11]. The DEVD-AFC cleavage reaction catalysed by caspase-3 and procaspase-3 processing reaction had the same optimum pH. The rate of fluorescent AFC production from the substrate DEVD-AFC by active caspase-3 was much faster than the rate of processing reaction of procaspase-3 at the optimum pH of 7.5. AFC production could be expressed as the rate of procaspase-3 processing, because procaspase-3 processing is the rate-determining step. Negative staining of SDS–polyacrylamide gel electrophoresis (PAGE)

*Corresponding author. Fax: +81 88 622 2503.
E-mail address: katunuma@tokushima.bunri-u.ac.jp (N. Katunuma).

Abbreviations: LPS, lipopolysaccharide; AFC, 7-amino-4-trifluoromethyl-coumarin; ML, mitochondria-lysosome; AST, aspartate aminotransferase; ALT, alanine aminotransferase; PAGE, polyacrylamide gel electrophoresis; LRF, lactoferrin releasing factor

0014-5793/$32.00
doi:10.1016/j.febslet.2006.05.057

for the activator sample was performed basically according to the method of Fernandez et al. [12]. The processing activities were assayed in the 78-kDa band eluents after removing SDS with renaturing buffer.

2.3. Detection of procaspase-3 activating protein using fluorescent reverse zymography

Our new double layer fluorescent reverse zymographic method was used for the detection of procaspase-3 activating proteins [21]. The activator sample was applied to a 15% polyacrylamide gel copolymerized with DEVD-AFC as the caspase-3 substrate, and the electrophoresis was performed at 13 mA for 120 min. After removing SDS from the gel with the renaturing buffer (2.5% Triton X-100), the gel was incubated with 100 μM procaspase-3 solution at 37 °C for 30 min. The fluorescent AFC band formed by caspase-3 was detected using a UV-transilluminator [13].

2.4. Determination of amino acid sequence of the activating protein of 78-kDa

The intramolecular sequences of the activating protein isolated from the Zn-negative staining SDS–PAGE was determined using an HP G1005A protein sequencing system according to the Majima's method [14]. The protein in the 78-kDa band was digested with lysyl-endopeptidase and the peptide fragments were separated with reverse-phase HPLC on a TSK gel ODS-120 T column (Tosoh) with a linear gradient of acetonitrile in 0.05% trifluoroacetic acid. The amino acid sequences of the main separated peptides were also determined using Majima's method [14].

2.5. Confocal immunohistochemical analysis of lactoferrin located in liver lysosomes

Confocal immunofluorescence analysis was performed on liver sections from C57BL/6 mice using FITC-labeled anti-lactoferrin pAb (Cappel, Turnhout, Belgium) and PE-labeled anti-Lamp-1 mAb (Santa Cruz Biotechnology Inc., Santa Cruz, CA).

2.6. Method of administration of D-galactosamine with LPS in vivo

Rat liver apoptosis was induced by D-galactosamine treatment using Muntane's method [8] by the intraperitoneal injection of D-galactosamine 0.5 g/kg or D-galactosamine 0.5 g/kg plus LPS 50 μg/kg. Twelve hours after the injection, the rats were sacrificed to prepare the livers.

2.7. Preparation of lysosomes and cytoplasmic fraction of rat liver

The rat liver was gently homogenized with a Teflon pestle in 0.25 M cold isotonic sucrose buffer. The suspension was centrifuged at $3500 \times g$ for 10 min at 4 °C to remove the nucleuses and cells. The supernatant was centrifuged at $25000 \times g$ for 20 min at 4 °C to prepare the lysosome-mitochondrial (ML) fraction, and then to prepare the cytoplasm fraction, the supernatant was further centrifuged at $100000 \times g$ for 60 min to remove the microsomes. To prepare pure lysosomes, a two-phase partition centrifugation method in the presence of 1 mM $CaCl_2$ was used [15]. The lysosomal fractions for the assay of procaspase-3 activation were extracted using a 40 μM digitonin solution with isotonic sucrose buffer.

2.8. Sample preparation for activity assay of the lysosomal procaspase-3 activating protein

The ML fractions of rat liver were extracted with 5 mL of digitonin solution. After concentration to 1 mL, 30 μL portion of the extract was applied to SDS gel to make SDS–PAGE. After removing the SDS, the 78-kDa fractions were eluted from the gel for determination of procaspase-3 activating activity or assay of the lactoferrin protein by the antibody. The activating activities were expressed as the AFC released nM/h/mg protein (cytoplasmic protein, lysosomal protein or SDS–PAGE band protein).

2.9. Statistical analysis

Values for expression are shown as means ± S.D. Quantitative differences between values were statistically analyzed by Dunnett's multiple comparison *t* test P values <0.01 were considered to be significant.

3. Results and discussion

3.1. Detection of procaspase-3 activating protein in the cytoplasm of D-galactosamine treated apoptotic liver cells

When D-galactosamine was administered intraperitoneally to rats, caspase-3 activity in the liver cytoplasm was elevated in a dose-dependent manner 12 h after injection and cotreatment with LPS enhanced the apoptosis dramatically, as shown in Table 1. The liver injury markers, aspartate aminotransferase (AST) and alanine aminotransferase (ALT), were strongly elevated in the serum. Therefore, the increases of caspase-3 may participate in D-galactosamine induced liver injury [11].

In order to elucidate the mechanism of caspase-3 elevation during the apoptosis, the activation factor of procaspase-3 in the treated liver cytoplasm was determined by the following procedure. Same amounts of cytoplasmic fraction and lyso-

Table 1
Elevation of caspase-3 in liver cytoplasm and translocation of lysosomal lactoferrin from lysosomes into cytoplasm in rat liver induced apoptosis by D-galactosamine

Treatments	Enzymes					
	In liver cytoplasm		In liver lysosomes		In serum	
	Caspase-3 (AFC nM/mg/hr)	Activator, 78 kDa (AFC nM/mg/h)	Activator, 78 kDa (AFC nM/mg/h)	Activator, 35 kDa (AFC nM/mg/h)	AST (IU/l)	ALT (IU/l)
Normal	76.50 ± 9.42	25.0 ± 18.6	612.6 ± 210	100.0	23.37 ± 3.69	4.15 ± 1.17
D-GalN (300 mg/kg)		180 ± 90.0	250.0 ± 150	95.0		
D-GalN (500 mg/kg)	1000.0 ± 360	322 ± 126.0	152.4 ± 60	110.0	247.37 ± 194.07	70.17 ± 51.15
D-GalN (700 mg/kg)		609 ± 40	20.0 ± 15	105.0		
LPS(50 μg/kg)	97.56 ± 21.65				23.33 ± 6.25	6.67 ± 1.25
D-GalN(500 mg) + LPS(50 μg/kg)	5159.73 ± 1250.37	1488.6 ± 576.9	≒0		2154.31 ± 598.02	525.94 ± 140.74

0.5 g/kg of the D-galactosamine plus 50 mg/kg of LPS was intraperitoneally injected to rats, and the 12 h after the injection, the rats were sacrificed. The procaspase-3 activating activities (lactoferrin) translocated from the lysosomes into the cytoplasm in the apoptotic hepatocyte were assayed using the method as follows. The quantitative amounts of the digitonin extracts of the lysosomes or the cytoplasm preparations were applied to make SDS–PAGE, and the procaspase-3 activating activities in the 78-kDa fractions and those in the 35-kDa fractions from the lysosomes, and also those from the cytoplasms were assayed at the same time. Furthermore, these activating protein amounts in the cytoplasm corresponded to the released lactoferrin protein amounts using ant lactoferrin antibody [18]. The activating activities were expressed as the AFC released nM/h/mg protein in the extracts of cytoplasmic protein or lysosomal protein. The reciprocal movements of the lactoferrin (procaspase-3 processing activities) in the lysosomes and the cytoplasm were observed in D-galactosamine dose-dependently. Data are shown as the means ± S.D.: $n = 3$–5, $^{*}P < 0.01$.

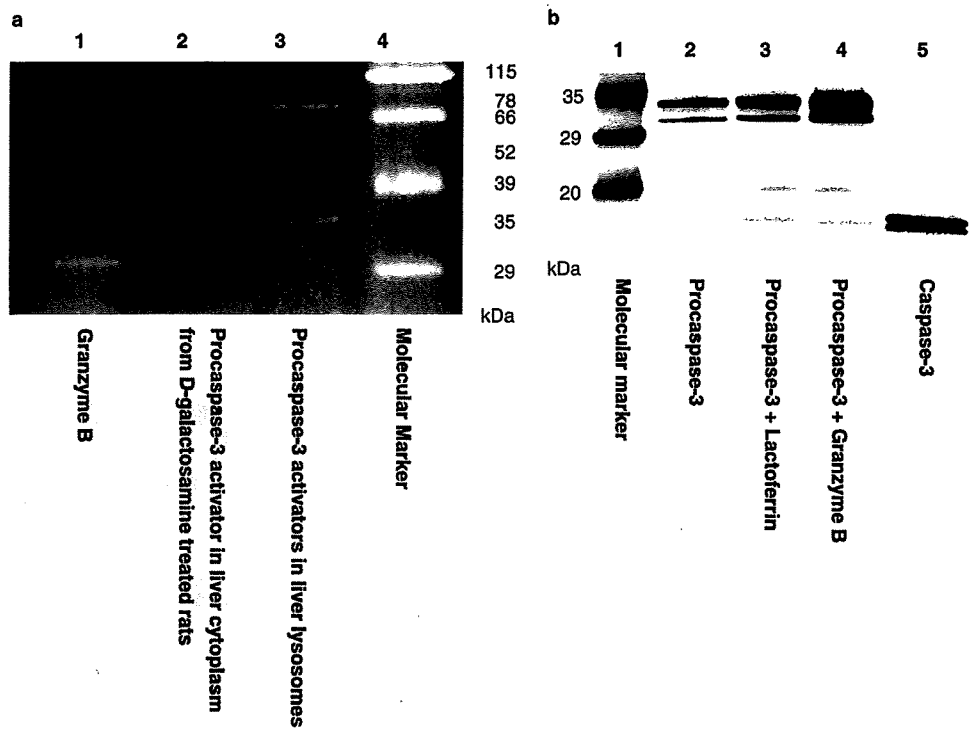

Fig. 1. (a) Detection of procaspase-3 activating proteins in rat liver treated with D-galactosamine using double-layer fluorescent reverse zymography. The procaspase-3 activating proteins were detected using Katunuma's double-layer fluorescent reverse zymography; the method is described in the text [13,21]. DEVD-AFC was used as a caspase-3 substrate. Lane 1: location of granzyme B as the procaspase-3 activating enzyme in the 32-kDa band. Lane 2: Procaspase-3 activating protein in the 78-kDa band was detected in the liver cytoplasm fraction of D-galactosamine treated rats. Lane 3: Procaspase-3 activating proteins in the digitonin extracts of liver lysosome from normal rats in the 78-kDa band which corresponds to the band of lactoferrin and the 35-kDa protein band which is unknown activating protein. (b) Procaspase-3 processing products by lactoferrin. SDS–PAGE gel was stained by Coomassie blue. The products of procaspase-3 processing mediated by lactoferrin were the same as those produced by granzyme B.

somal extract of liver were applied separately to SDS gels and electrophoresis was performed. After removing the SDS from the PAGE with renaturing buffer, the procaspase-3 processing activities in the eluents were detected in the 78-kDa fraction and the 35-kDa fraction using caspase-3 formation from recombinant procaspase-3. The procaspase-3 activating protein in the 78-kDa fraction was increased in the cytoplasm and the activity in the lysosomes was decreased in a reciprocal manner, as shown in Table 1. Sufficient amounts of procaspase-3 were present in the normal cytoplasm, but active caspase-3 was not detected in the normal cytoplasm. These data suggest that the procaspase-3 activating protein is originally located in the lysosomes under normal conditions and that only the 78-kDa activating protein was released into the cytoplasm by D-galactosamine administration.

We then purified the 78-kDa activating protein from the liver lysosomes to allow identification. The partially purified activating protein from the digitonin extracts of liver lysosomes was applied to SDS gels to separate the proteins. Two kinds of activating proteins with molecular weights of 78-kDa and 35-kDa were detected using fluorescent reverse zymography for processing protease detection [13,21], as shown in Fig. 1(a) in lane 3. The 78-kDa band corresponds to recombinant lactoferrin, and the 35-kDa band is an unknown activating protein. The 35-kDa factor was not detected in the cytoplasm of the apoptotic liver, therefore, the 35-kDa factor does not participate in the apoptosis.

3.2. *Purification and identification of the 78-kDa lysosomal activating protein as lactoferrin*

A procaspase-3 activating protein was extracted with a 40 μM digitonin isotonic sucrose buffer from the purified lysosomes of bovine liver. The specific activity of the procaspase-3 processing enzyme in the digitonin extracts was 2.5 nmol AFC/h/μg protein (formed from DEVD-AFC). The extracted protein was fractionated with 40–60% ammonium sulfate and then heat treated at 70 °C for 1 min. The supernatant was further fractionated with 40–50% ethanol at −20 °C. The fraction was subsequently subjected to column chromatography using Superdex G75, Mono Q and then Hydroxyapatite CHT5-I BIO-RAD. The specific activity of the final active fraction was about 100 nmol AFC/h/μg protein. The purity was increased about 40 times compared with that of the digitonin extracts. The purified sample had about the same activating activity as that of the recombinant pure lactoferrin. The purified fraction showed almost a single protein on the SDS–PAGE.

The intramolecular amino acid sequence of the purified 78-kDa activating protein eluted from the negative zinc staining band in the SDS–PAGE was determined [12]. The sample was hydrolyzed with lysyl-endopeptidase and the peptides produced were separated using reversed-phase HPLC. The amino acid sequences of the two different parts of the separated peptides were determined. The amino acid sequences of these two peptides were completely identical with those of the corresponding parts of recombinant bovine lactoferrin. The amino

acid sequences of these two domains from the purified sample were H_{435}-P_{444} (n-H-S-S-L-D-C-V-L-R-P-c) and N_{653}-E_{661} (n-N-L-L-F-N-D-N-T-E-c). The molecular weight (78-kDa) and the isoelectric point (5.4–5.7) of the purified activating protein were the same as those of the recombinant bovine lactoferrin. The processing product of procaspase-3 by the 78-kDa protein was the same as that by recombinant lactoferrin as demonstrated in Fig. 1(b). The same processing products of procaspase-3 by granzyme B were demonstrated.

3.3. Subcellular localization of lactoferrin in liver lysosomes

A two-phase Ficoll partition centrifugation method in 1 mM $CaCl_2$ was used to determine the subcellular localization of the activating protein in rat liver [15]. The activating activity was detected only in the lysosomal fraction, coinciding with the location of cathepsin L, while the activity was not detected in the swollen mitochondrial fraction, coinciding with glutamic dehydrogenase (data not shown). The confocal immunohistochemical staining of mouse liver, using a monoclonal anti-lactoferrin antibody and a PF-labeled anti-Lamp-1 antibody as lysosomal markers, was used to determine the subcellular localization of the lactoferrin (see Section 2). The lactoferrin was detected only in the lysosomal particles located in the cell membrane area, as Fig. 2 shows.

3.4. Activation mechanism of procaspase-3 by lactoferrin

The activation mode of the procaspase-3 processing reaction mediated by pure lactoferrin was analyzed. Procaspase-3 was originally processed slowly via autocatalytic reaction in Tris–HCl buffer at pH 7.5 and 37 °C in vitro, and 1×10^{-7} M lactoferrin strongly accelerated the autocatalytic processing to several-fold, as shown in Fig. 3(a). The procaspase-3 processing rate mediated by 1×10^{-6} M lactoferrin was about 7000–8000 nM AFC formed per hour, while the autocatalytic rate was about 1000–1600 nM AFC formed per hour. Specific activity of procaspase-3 processing reaction catalyzed by lactoferrin was 432 nM AFC formed/h/mg protein, while that by granzyme B was 515 nM AFC formed/h/mg. Both catalytic activities showed about the same level. The lactoferrin mediated procaspase-3 activating reaction was not inhibited by various cysteine protease inhibitors, including E-64 or serine protease inhibitors, and anti-granzyme B antibody also did not inhibit the activation reaction (data abbreviated). Since both apo-lactoferrin and holo-lactoferrin had the same activation function and 1×10^{-7} M lactoferrin showed the enough activation (Fig. 3(b)), the iron atom itself and the domains of the iron atom binding did not participate in this activation reaction. The processing products of recombinant procaspase-3 mediated by lactoferrin were the same as those mediated by granzyme B by Western blotting using the anti-caspase-3 antibody as shown in Fig. 1(b).

With regard to the activating mechanism of procaspase-3 processing by the lactoferrin, a lactoferrin–procaspase-3 complex may be formed as an intermediate step. The lactoferrin may play a chaperone-like role to alter the tertiary structure of the procaspase-3 and render it more susceptible to being processed. The binding affinity for making the complex was shown in Fig. 3(c), and the K_m is about 1×10^{-11} M. The lactoferrin did not have any effect on the caspase-3 assay reaction. The domain which participates in the binding of procaspase-3 to the lactoferrin molecule was estimated to be Y_{679}-K_{695} (YEKYLGPQYVAGITNLK) in lactoferrin. We reported previously that this domain was an inhibitory site of the

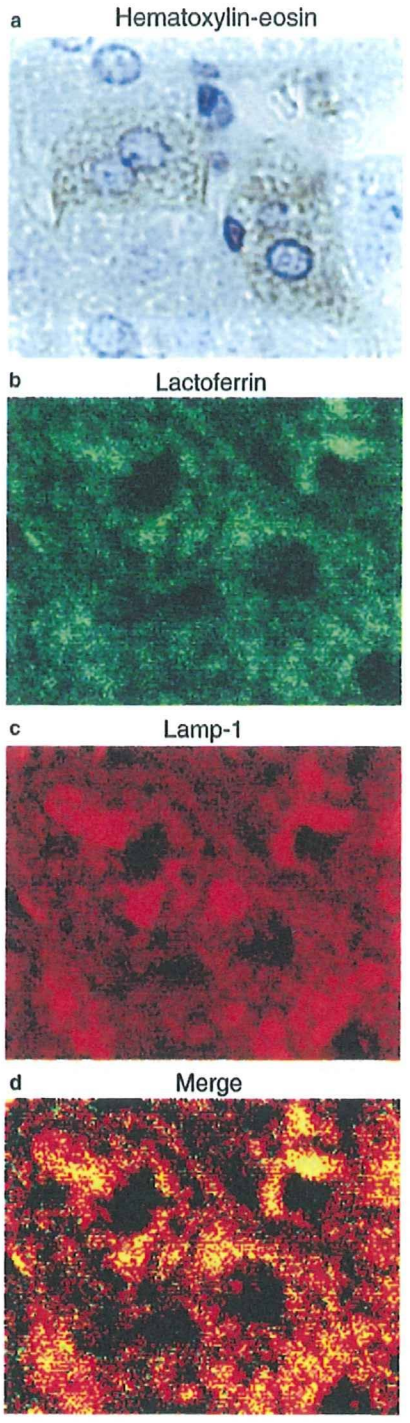

Fig. 2. Subcellular localization of lactoferrin in rat liver using confocal immunohistochemical staining. (a) Hematoxylin-eosin staining of hepatocytes. (b) Lactoferrin localization in lysosomes using an anti-lactoferrin antibody in green. (c) Lysosome staining by PF-labeled-anti-Lamp-1 antibody in red. (d) Merged profile of lactoferrin and lysosomal marker Lamp-1. The lactoferrin was stained in the lysosomes located in the cell membrane area.

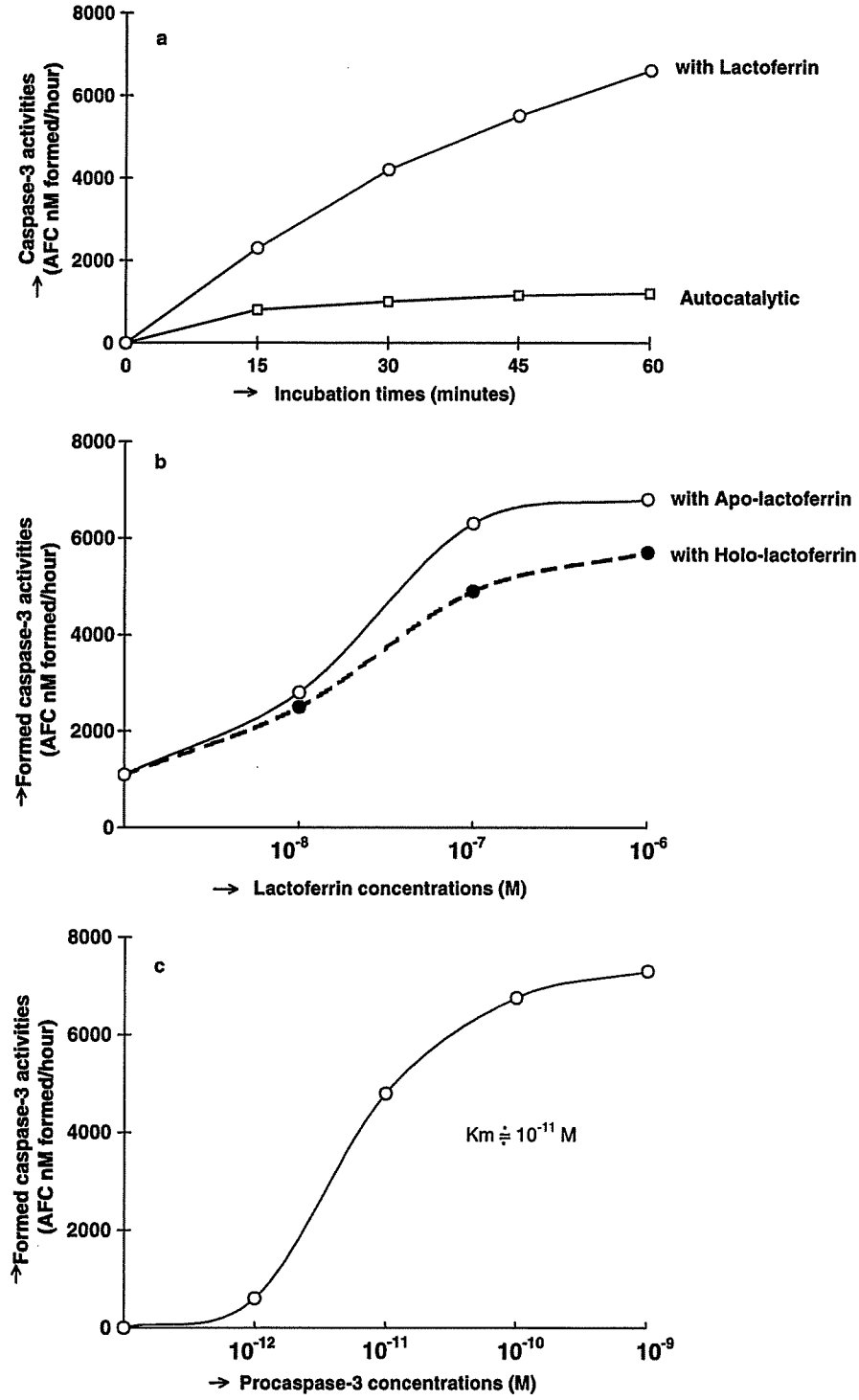

Fig. 3. Activating mechanisms of procaspase-3 processing reaction mediated by lactoferrin. The procaspase-3 processing activity was assayed by the formed caspase-3 activity and the formed caspase-3 activities from procaspase-3 are expressed as AFC formed nM/h in the vertical axis. Panel (a): Reaction time course of procaspase-3 processing with lactoferrin. Panel (b): Dose-dependent activations of the procaspase-3 processing reaction mediated by holo-lactoferrin or apo-lactoferrin. Apo-lactoferrin was prepared from holo-lactoferrin by the treatments at pH 2.0. The iron atoms were released into the supernatant and no iron atoms were detected in the precipitated lactoferrin. Panel (c): Kinetical studies of the affinity of procaspase-3 for lactoferrin and the K_m value.

lactoferrin for cysteine proteases [16]. This domain is highly homologous with a common active site of the cystatin family. The synthetic peptide Y_{679}-K_{695} strongly inhibited not only the activation reaction of the processing mediated by lactoferrin, but also the autocatalytic processing reaction, as shown in Fig. 4. This peptide may disturb the binding of procaspase-3

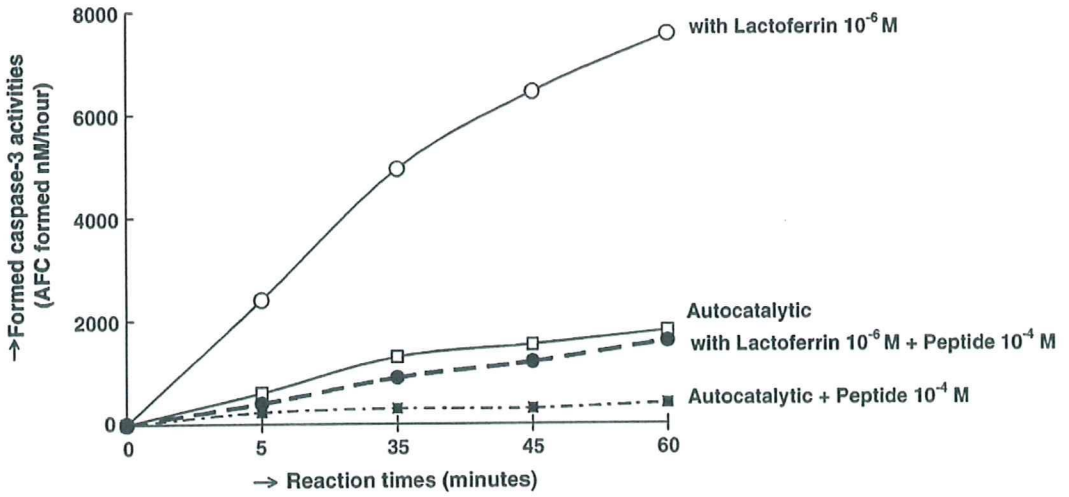

Fig. 4. Inhibition profiles of procaspase-3 processing reaction mediated by lactoferrin by synthetic peptide, Y_{679}-K_{695}, in the domain of lactoferrin molecule. Lactoferrin concentration of 1×10^{-6} M as an activator and synthetic peptide concentration of 1×10^{-4} M as the inhibitor were used. The procaspase-3 processing reaction mediated by 1×10^{-6} M lactoferrin (○–○) and inhibited by 1×10^{-4} M of the peptide (●···●) are shown in this panel. Autocatalytic processing (□–□) and inhibition with 1×10^{-4} M peptide (■···■) are also shown.

to lactoferrin. Therefore, the domain Y_{679}-K_{695} of the lactoferrin may play an important role in the acceleration function by participating in the binding of procaspase-3 to lactoferrin. To explain the practical allosteric structural changes, the X-ray co-crystallographic analysis of these complexes is required. We previously reported a similar type of chaperone-like functioning protein, a chondroitin-sulfate proteoglycan, which is a potent enhancer of the autoprocessing of procathepsin L to form the active mature cathepsin L [17]. We propose that these kinds of specific accelerator proteins, or "enzymoids", may participate in various post-translational processing reactions in general.

3.5. A new apoptosis cascade mediated by lysosomal lactoferrin

To confirm the translocation of the lactoferrin, the lactoferrin released in the cytoplasm was assayed quantitatively with antibodies to lactoferrin using Sanchez's method [18]. The lactoferrin released in the cytoplasm increased to 7 μg/mL of cytoplasm upon treatment with 700 mg/kg D-galactosamine, while no lactoferrin was detected in the normal liver cytoplasm. It is possible to consider that the lactoferrin located in the lysosomes was released into the cytoplasm by D-galactosamine administration dose-dependently in vivo as shown in Table 1, although the releasing mechanisms are not known at the present. The released procaspase-3 activating activity in

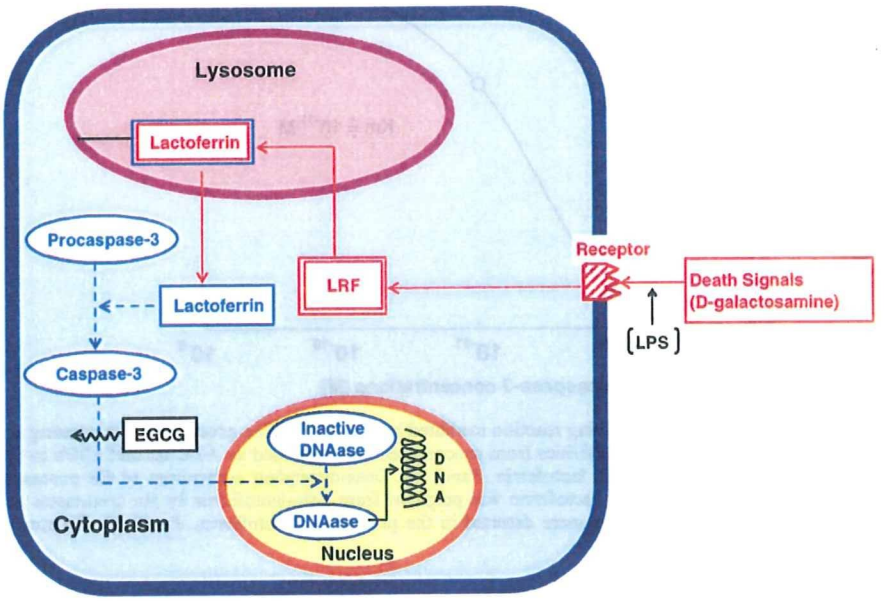

Fig. 5. Schematic illustration of a new apoptosis cascade mediated by lysosomal lactoferrin. Solid red line; the death signal transduction induced by D-galactosamine. Dotted blue line; a new apoptosis cascade mediated by lysosomal lactoferrin. LRF; unknown lactoferrin releasing factor.

the cytoplasm by D-galactosamine plus LPS treatment was 5000–6000 AFC nM/h, this activity is corresponding to the activity by 10^{-6}–10^{-7} M of lactoferrin (calculated by Fig. 3(b)). This amount (concentration) is enough to activate procaspase-3 in vitro. Sufficient amounts of procaspase-3 are located in the normal liver cytoplasm, but caspase-3 was not present in the normal cytoplasm. As a model experiment, the caspase-3 activity (DEVD-AFC cleaving activity) in a normal liver cytoplasm preparation was found to be strongly enhanced by the addition of recombinant lactoferrin in vitro. We reported in our previous papers that the caspase-3 activity in the normal liver cytoplasm was enhanced by the addition of digitonin extracts of lysosomes in vitro [5,6]. The activities of other known caspases [6,8,11,13], which are the proteolytic signal transduction caspases, were not changed by the D-galactosamine treatment (data not shown). When a suitable death signal was added, the corresponding activating protein was translocated from the different organelles into the cytoplasm, resulting in increases in caspase-3 mediated apoptosis, in general [1]. The releasing mechanism of lysosomal lactoferrin by D-galactosamine treatment is not known. Quintero et al. reported that prostaglandin E1 protection against apoptosis induced by D-galactosamine is not related to the modulation of intracellular free radical production in primary culture of rat hepatocyte [19]. However, we have not any direct evidences on the releasing mechanisms of lysosomal lactoferrin into cytoplasm by D-galactosamine induced hepatocyte apoptosis. Fujita et al. reported that lactoferrin stimulated the apoptosis of azoxymethane-induced tumors and the elevation of active forms of caspases-3 and 8. But little is known about the mechanisms at the molecular level. The problem of this report is that the lactoferrin was administrated perorally with diet, it is difficult to consider that the 72-kDa lactoferrin is effectively absorbed from intestine [20]. The caspase-3 activity was dramatically elevated in the cytoplasm of D-galactosamine induced apoptotic hepatocytes and administration of epigallo-catechin gallate which was strong inhibitor for caspase-3 activity suppressed the elevation of caspase-3 activity in the cytoplasm and protected the hepatocyte apoptosis [11]. Our proposed new apoptotic cascade mediated by lysosomal lactoferrin is illustrated schematically in Fig. 5.

Acknowledgements: This work was supported by the Grants-in-aid from the Japanese Ministry of Education, Sciences and Culture. We thank Professor Guy Salvesen for his useful advice and thank Rika Takahashi for her valuable help in preparing this manuscript.

References

[1] Salvesen, G.S. and Dixit, V.M. (1997) Caspases, intracellular signaling by proteolysis. Cell 91, 443–446.
[2] Liu, X., Kim, C.N., Yang, J., Jemmerson, R. and Wang, X. (1996) Induction of apoptotic program in cell-free extracts: requirement for dATP and cytochrome *c*. Cell 86, 147–157.
[3] Kluck, R.M., Bossy-Wetzel, E., Green, D.R. and Newmeyer, D.D. (1997) The release of cytochrome *c* from mitochondria: a primary site for Bcl-2 regulation of apoptosis. Science 275, 1132–1136.
[4] Li, P., Nijhawan, D., Budihardjo, I., Srinivasula, S.M., Ahmad, M., Alnemri, E.S. and Wang, X. (1997) Cytochrome *c* and dATP-dependent formation of Apaf-1/caspase-9 complex initiates an apoptotic protease cascade. Cell 91, 479–489.
[5] Ishisaka, R., Utsumi, T., Yabuki, M., Kanno, T., Furuno, T., Inoue, M. and Utsumi, K. (1998) Activation of caspase-3 like protease by digitonin-treated lysosomes. FEBS Lett. 435, 233–236.
[6] Ishisaka, R., Utsumi, T., Kanno, T., Arita, K., Katunuma, N., Akiyama, J. and Utsumi, K. (1999) Participation of a cathepsin L-type protease in the activation of caspase-3. Cell Struct. Funct. 24, 465–470.
[7] Katunuma, N., Murata, E., Le, Q.T., Hayashi, Y. and Ohashi, A. (2004) New apoptosis cascade mediated by lysosomal enzyme and its protection by epigallo-catechin gallate. Adv. Enzyme Regul. 44, 1–10.
[8] Muntane, J., Montero, J.L., Marchal, T., Perez-Seoane, C., Lozano, J.M., Fraga, E., Pintado, C., de la Mata, O. and Mino, G. (1998) Effect of PGE_1 on TNF-α status and hepatic D-galactosamine-induced apoptosis in rats. J. Gastroent. Hepatol. 13, 197–207.
[9] Galanos, C., Freudenberg, M.A. and Reutter, W. (1979) Galactosamine-induced sensitization to the lethal effects of endotoxin. Proc. Natl. Acad. Sci. USA 76, 5939–5943.
[10] Thornberry, N.A., Bull, H.G., Calaycay, J.R., Chapman, K.T., Howard, A.D., Kostura, M.J., Kostura, M.J., Miller, D.K., Molineaux, S.M., Weidner, J.R., Aunins, J., Elliston, K.O., Ayala, Jm., Casano, F.J., Chin, J., Ding, G.J.-F., Egger, L.A., Gaffney, E.P., Limjuco, G., Palyha, O.C., Raju, S.M., Ralond, A.M., Salley, J.P., Yamin, T.T., Lee, T.D., Shively, J.E., MacCross, M., Mumford, R.A., Schumidt, J.A. and Tocci, M.J. (1992) A novel heterodimeric cysteine protease is required for interleukin-1 beta processing in monocytes. Nature 356, 768–774.
[11] Katunuma, N., Ohashi, A., Sano, E., Ishimaru, N., Hayashi, Y. and Murata, E. (2006) Catechin derivatives: specific inhibitor for caspases-3, 7 and 2, and the prevention of apoptosis at the cell and animal levels. FEBS Lett. 580, 741–746.
[12] Fernandez-Patron, C., Castellanos-Serra, L. and Rodriguez, P. (1992) Reverse staining of sodium dodecyl sulfate polyacrylamide gels by imidazole-zinc salts: sensitive detection of unmodified proteins. Biotechniques 12, 564–573.
[13] Le, Q.T., Ohashi, A., Hirose, S. and Katunuma, N. (2005) Reverse zymography using fluorogenic substrates for protease inhibitor detection. Electrophoresis 26, 1038–1045.
[14] Majima, E., Ishida, M., Miki, S., Shinohara, Y. and Terada, H. (2001) Specific labeling of the bovine heart mitochondrial phosphate carrier with fluorescein 5-isothiocyanate: roles of Lys185 and putative adenine nucleotide recognition site in phosphate transport. J. Biol. Chem. 276, 9792–9799.
[15] Osada, J., Aylagas, H., Sanchez-Prieto, J., Sanchez-Vegazo, I. and Palacios-Alaiz, E. (1990) Isolation of rat liver lysosomes by a single two-phase partition on dextran/polyethylene glycol. Anal. Biochem. 185, 249–253.
[16] Ohashi, A., Murata, E., Yamamoto, K., Majima, E., Sano, E., Le, Q.T. and Katunuma, N. (2003) New functions of lactoferrin and β-casein in mammalian milk as cysteine protease inhibitors. BBRC 306, 98–103.
[17] Kihara, M., Kakegawa, H., Matano, Y., Murata, E., Tsuge, H., Kido, H. and Katunuma, N. (2002) Chondroitin sulfate proteoglycan is a potent enhancer in the processing of procathepsin L. Biol. Chem. 383, 1925–1929.
[18] Sanchez, L., Aranda, P., Perez, M.D. and Calvo, M. (1988) Concentration of lactoferrin and transferrin throughout lactation in cow's colostrum and milk. Biol. Chem. Hoppe Seyler 369, 1005–1008.
[19] Quintero, A., Pedraza, C.A., Siendones, E., Kamal ElSaid, A.M., Colell, A., Garcia-Ruiz, C., Montero, J.L., De la Mata, M., Fernandez-Checa, J.C., Mino, G. and Muntane, J. (2002) PGE_1 protection against apoptosis induced by D-galactosamine is not related to the modulation of intracellular free radical production in primary culture of rat hepatocytes. Free Radic. Res. 36, 345–355.
[20] Fujita, K., Matsuda, E., Sekine, K., Iigo, M. and Tsuda, H. (2004) Lactoferrin enhances Fas expression and apoptosis in the colon mucosa of azoxymethane-treated rats. Carcinogenesis 25, 1961–1966.
[21] Katunuma, N., Le, Q.T., Miyauchi, R. and Hirose, S. (2005) Double-layer fluorescent zymography for processing protease detection. Anal. Biochem. 347, 208–212.

FEBS Letters 580 (2006) 741–746

Catechin derivatives: Specific inhibitor for caspases-3, 7 and 2, and the prevention of apoptosis at the cell and animal levels

Nobuhiko Katunuma[a,*], Atsushi Ohashi[a], Etsuko Sano[a], Naozumi Ishimaru[b], Yoshio Hayashi[b], Etsuko Murata[a]

[a] *Tokushima Bunri University, Institute for Health Sciences, 180 Nishihamabouji, Yamashiro-cho, Tokushima 770-8514, Japan*
[b] *The University of Tokushima Graduate School, Department of Oral Molecular Pathology, Institute of Health Biosciences, 3-18-15 Kuramoto-cho, Tokushima 770-8504, Japan*

Received 6 October 2005; revised 22 December 2005; accepted 28 December 2005

Available online 6 January 2006

Edited by Vladimir Skulachev

Abstract **Tea-catechin derivatives are shown to inhibit activities of caspases-3, 2 and 7 in vitro, and prevented experimental apoptosis at the cell and animal levels. Epigallo-catechin-gallate showed the strongest inhibition at 1×10^{-7} M to these caspases, but cysteine cathepsins and caspase-8 were not inhibited. Caspase-3 inhibition showed a 2nd-order allosteric-type, but the inhibition of caspases-2 and 7 showed a non-competitive-type. The apoptosis-test using cultured HeLa cells was inhibited by these catechins. In rat hepatocytes, apoptosis was induced by D-galactosamine in vivo. In this case, caspase-3 activity in the cytoplasm, the serum aminotransferases and dUTP nick formation detected by TUNNEL-staining were effects, and these elevations were suppressed by administration of catechin.**

Keywords: Catechin; Caspase-3; Apoptosis; D-Galactosamine; Serum aminotransferase

1. Introduction

Various pharmacological functions of tea-catechin derivatives have been extensively studied in recent years. Their anti-oxidant effects are well established; in addition, the possibility for prevention of oncogenesis by tea-catechins from the aspect of epidemiological statistics has been advocated. However, no reasonable explanation exists for the prevention of oncogenesis at the molecular level (see Section 4). The direct effect of tea-catechins on specific caspases with respect to apoptosis has not yet been reported. The synthetic inhibitors of substrate analogues for caspases have been reported; however, natural inhibitors have not been identified. Allosteric inhibition of caspase-3 by synthetic inhibitors was reported by Hardy et al., therefore the tertiary structures of caspases are flexible (see Section 4) [11]. We have previously shown that some tea-catechin derivatives strongly inhibited caspases-3, 2 and 7, in vitro and in vivo [1,2,5–9].

The inhibition of cultured HeLa cell apoptosis test, which is reported by Wells et al., was studied [4]. Liver injury induced by D-galactosamine with lipopolysaccharide (LPS) in vivo is well characterized to induce hepatocyte apoptosis within the pathological field, assessed by TUNNEL-staining and DNA fragmentation [1–4]. The activity of caspase-3 in the liver cytoplasm was significantly elevated, and aspartate (AST) and alanine (ALT) aminotransferases in the serum were also significantly elevated in the D-galactosamine induced apoptotic liver. These increases were suppressed by epigallo-catechin-gallate (EGCG) in vivo. EGCG is the main component of green tea. The specific inhibition of activities of caspases-3, 2 and 7 by tea-catechin derivatives in vitro and the prevention of liver cell apoptosis in vivo are reported in this paper.

2. Materials and methods

2.1. Materials

Recombinant human caspases-3, 7, 8 and 2 were purchased from Bio-Vision Co. Catechin derivatives were purchased from Wako Co. Cathepsin B and L were purchased from Sigma.

2.2. Methods

2.2.1. Inhibition assays of caspases-3, 7, 2 and 8 activities by catechin derivatives. An established method for the assay of activities of caspase-3 and caspase-7 was used [9], using the recombinant pure caspases and DEVD-AFC as the substrate. Ac-IETD-MCA was used for caspase-8 and AC-VDVAD-MCA was used for caspase-2. Enzyme activity was expressed as the released AFC (or MCA) formed nM/h/mg protein.

2.2.2. Cell-free apoptosis test using cultured HeLa cell S-100. The apoptosis assay system reported by Wells et al. is composed of cultured HeLa cell cytoplasm S-100 (4 mg protein/ml), cytochrome *c* (80 μM) and Ac-DEVD-MCA (40 μM) as the substrate for formed caspase-3 [12]. Preparation of S-100 from cultured HeLa cells was followed using the method described by Wells and Nguyen [12]. Following incubation at 37 °C for 40 min, the released fluorescent MCA in the S-100 fraction was assayed as formed caspase-3 from procaspase-3 in the S-100. Caspase-3 activity without addition of cytochrome *c* was used as the negative control.

2.2.3. Administration method of D-galactosamine and tea-catechin derivatives in rats. Liver apoptosis was induced according to Muntane's method, by intraperitoneal injection of D-galactosamine [3,4]. A single dose of D-galactosamine was administered intraperitoneally

*Corresponding author. Fax: +81 88 622 2503.
E-mail address: katunuma@tokushima.bunri-u.ac.jp (N. Katunuma).

Abbreviations: AST, aspartate aminotransferase; ALT, alanine aminotransferase; EGCG, epigallo-catechin gallate; ECG, epi-catechin gallate; CG, catechin gallate; EC, epi-catechin; EGC, epigallo-catechin; C, catechin; GC, gallo-catechin; G, gallate; LPS, lipopolysaccharide; TdT, terminal transferase; MCA, methyl coumaryl amide

0014-5793/$32.00
doi:10.1016/j.febslet.2005.12.087

(0.5 g/kg), and rats were sacrificed 12 h after the injection. Two doses of EGCG with 50 μg/kg of LPS were administered intraperitoneally at 1 h before and after the D-galactosamine administration. EGCG was further administered twice at 3-h intervals.

2.2.4. Preparation of liver cytoplasm for assay of caspase-3 activity. Liver cytoplasm fraction for caspase-3 activity assay was prepared by sequential centrifugation method for cell organelle separation according to a method described by Fleisher and Kervina [16].

2.2.5. TdT-mediated dUTP nick end labeling (TUNNEL) assay. Apoptotic cells were detected in sections using the in situ Apoptosis Kit (Takara Kyoto, Japan). Frozen sections of liver tissues were fixed in 3% paraformaldehyde, incubated with protease K (20 μg/ml) for 10 min, and then presoaked in terminal transferase (TdT) buffer (0.5 μM/L cacodylate, 1 μM/L CoCl, 0.5 μM/L dithiothreitol, 0.05% bovine serum albumin, and 0.15 M/L NaCl) for 10 min. Sections were incubated for 1 h at 37 °C in 25 ml of TdT solution, containing 1× terminal transferase buffer, 0.5 nM of biotin-dUTP, and 10 U of TdT. After the TdT reaction, sections were soaked in TdT blocking buffer (300 nM/L NaCl and 30 mM/L tri-sodium citrate-2-hydrate), incubated with HRP-conjugated streptavidin for 30 min at room temperature, and developed for 10 min in phosphate-buffered citrate (pH 5.8) containing 0.6 mg/ml DAB. Nuclei were counterstained with hematoxylin.

3. Results

3.1. Inhibition of caspase-3 activity by various catechin derivatives in vitro

Caspase-3 plays a central role as an executive enzyme of apoptosis in the final step of various apoptotic cascades [5–9].

Table 1
Comparison of inhibition of caspase-3 activity in vitro and the apoptosis test using cultured HeLa cells by tea-catechin derivatives

Catechin Derivatives	*In vitro* 50% Inhibition of caspase-3	HeLa cell apoptosis test 50% inhibition of apoptosis test
Epigallo-Catechin Gallate 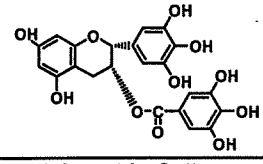	1×10^{-8} M	1×10^{-6} M
Epi-Catechin Gallate 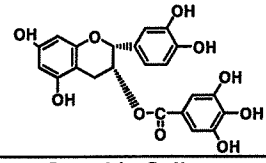	1×10^{-7} M	1×10^{-4} M
Catechin Gallate 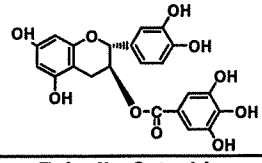	1×10^{-6} M	5×10^{-4} M
Epigallo-Catechin 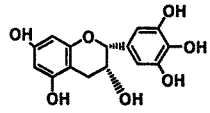	1×10^{-6} M	5×10^{-4} M
Epi-Catechin 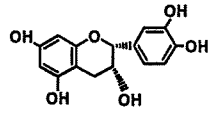	1×10^{-6} M	5×10^{-4} M
Catechin Gallate 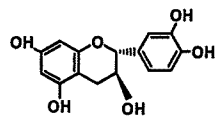	Gallo-Catechin 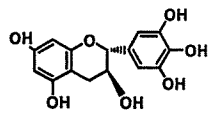	Gallic Acid 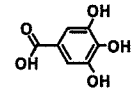	No Inhibitions by 1×10^{-4} M

The left-hand column shows the concentrations of catechin derivatives inducing 50% inhibition of caspase-3 activity in vitro. The right-hand column shows the 50% inhibition of the apoptosis test units of cultured HeLa cells. The assay methods are described in the text [10,11]. The 50% inhibition concentrations of various catechin derivatives are illustrated ($n = 3$, the mean ± S.E.M. with $^{*}P < 0.01$).

Caspase-3 activity was completely inhibited by EGCG at 1×10^{-7} M and was inhibited to 50% at 1×10^{-8} M in vitro. Epi-catechin gallate (ECG) showed 50% inhibition at 1×10^{-7}M, and catechin gallate (CG), epi-catechin (EC) and epigallo-catechin (EGC) had induced inhibition at 1×10^{-6} M. Catechin (C), gallo-catechin (GC) and gallate (G) showed no inhibition as Table 1 shows. The stereo-binding form of –OH to the catechin-ring should be an epi-structure to display inhibitory activity. The presence of either component, catechin gallate (CG) and/or epi-form catechin (EC), is essential.

Relationship of velocity and substrate concentration of caspase-3 in the presence of EGCG showed a typical sigmoidal curve and the Lineweaver–Burk relationship did not give a straight line, but showed a logarithmic curve. When the abscissa was taken as $1/[S]^2$, the logarithmic curve changed to a straight line (Fig. 1A). The inhibition kinetics of these catechin derivatives appear to be a 2nd-order sigmoidal allosteric inhibition as follows:

$$1/v = Km/V(1/[S]^2) + 1/V.$$

The other four effective catechin derivatives, such as ECG, CG, EC and EGC, also showed the same type of allosteric inhibition to caspase-3 as that by EGCG (figures are abbreviated).

The binding site of the catechins appeared to be different from the substrate-binding site. The allosteric nature of caspase-3 using synthetic inhibitors was reported by Hardy et al. [11] (see Section 4). The molecular weight of caspase-3 did not appear to change in the presence of EGCG and/or substrate using Superdex G-75. Therefore, polymerization or depolymerization was not observed using these allosteric inhibitors (data not shown).

3.2. Inhibitions of activities of caspases-7 and 2 activities by EGCG in vitro

Caspases-7 and 2 are also known to participate in various apoptosis cascades. The activities of caspases-7 and 2 were also strongly inhibited by EGCG, and the 50% activities were inhibited at 1×10^{-6} M. However, the mode of inhibitions of caspases-7 and 2 were different from that of caspase-3. The V_{max} decreased in the presence of EGCG and the Lineweaver–Burk relationship showed a non-competitive type inhibition (Fig. 1B and C). The binding site to EGCG is the same as the substrate-binding site or located near the active site. Caspase-8, cathepsins B and L, which are the same cysteine proteases, were not inhibited at 1×10^{-5} M of EGCG. Therefore, the inhibitions of caspases are not due to an attack to the active site –SH of these enzymes by the scavenger effect of catechins.

3.3. Inhibition of caspase-3 in HeLa cell apoptosis test induced by cytochrome c by EGCG

Wells et al. developed a cell-free apoptosis test using cultured HeLa cells [12]. The S-100 prepared from cultured HeLa cell cytoplasm contains sufficient amounts of procaspase-3 and the activating enzyme system except cytochrome *c*. Caspase-3 activity in the S-100 increased following the addition of cytochrome *c*, as shown in Fig. 2. The 70% of the apoptosis unit was inhibited by EGCG at a concentration of 1×10^{-5} M. The strengths of suppression by the various catechin derivatives were in the same order as the inhibitions of caspase-3 activity in vitro, as shown in Table 1.

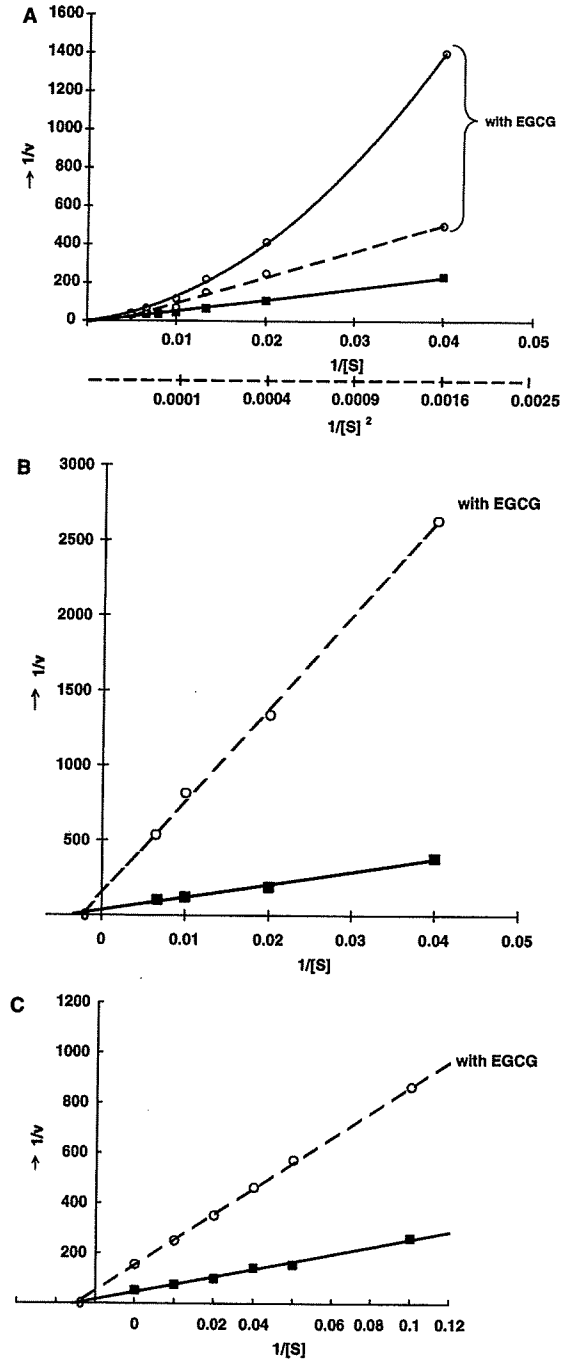

Fig. 1. Mode of inhibitions of caspase-3, 2 and 7 by EGCG in Lineweaver–Burk relationship. (A) Caspase-3 inhibition by 1×10^{-7} M of EGCG. The $1/v$ values to the $1/[S]$ in the presence of EGCG are expressed as open circles with a thin solid line (O–O). The $1/v$ values to the $1/[S]$ in the absence of EGCG are illustrated as closed squares with a solid line. The $1/v$ values to the $1/[S]^2$ illustration in the presence of EGCG are expressed as open circles with a broken line (O---O). (B) and (C) Caspase-2 or 7 inhibition by 1×10^{-6} M of EGCG. The activities in the absence of EGCG are illustrated as solid line with a solid line and the activities in the presence of EGCG are illustrated as open circles with a broken line. (B) shows caspase-2 inhibition by EGCG; the Lineweaver–Burk relationship. (C) shows caspase-7 inhibition by EGCG. All symbols and lines are the same as those in (B).

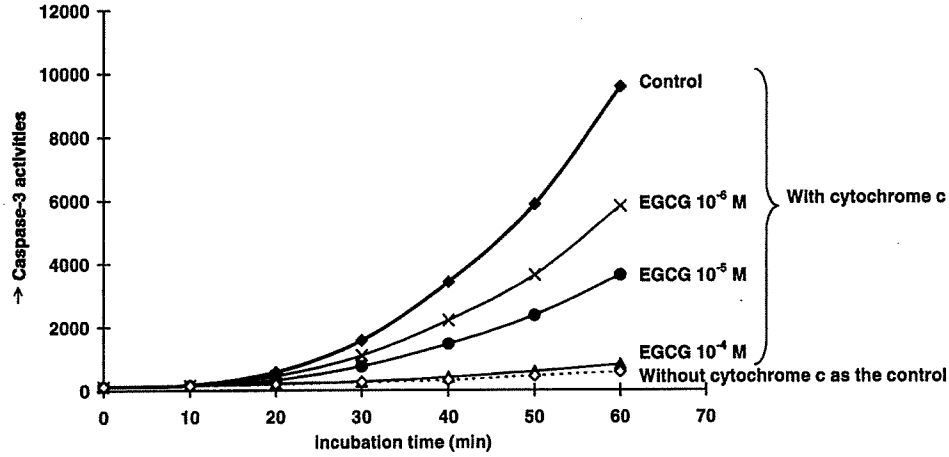

Fig. 2. Inhibition of caspase-3 activities in apoptotic test using cultured HeLa cells induced by cytochrome *c* by EGCG. Caspase-3 inhibition in S-100 of cultured HeLa cells by various catechin derivatives was assayed using Nguyen and Wells' apoptosis test as shown in Table 1, right panel [12]. The inhibitory activities by various catechin derivatives are compared as 50% inhibition concentrations as shown in Table 1, in left panel. The catechin derivatives added were expressed as the final concentrations in the S-100 fraction. All data are the means ± S.E.M. ($n = 5$) with $^{*}P < 0.01$.

3.4. Liver apoptosis induced by D-galactosamine plus LPS, and its prevention by EGCG in vivo

Sufficient amounts of procaspase-3 are present and active caspase-3 is not present in the normal hepatocyte cytoplasm. However, procaspase-3 in the cytoplasm is activated to form active caspase-3 by the effective apoptotic signal. It is well known within the pathological field that hepatocyte injury induced by D-galactosamine results in hepatocyte apoptosis, as assessed by the TUNNEL-staining and the DNA ladder formation [3,4,10].

(1) Elevations of liver caspase-3 activity and serum aminotransferases in D-galactosamine induced hepatocyte apoptosis, but were prevented by cotreatment with EGCG, as shown in Table 2. The both elevations were prevented by cotreatment with EGCG in a dose-dependent manner, and treatments with 50 mg/head EGCG suppressed the activity to the normal level. Furthermore, the macroscopic liver profile was protected and resembled to normal level.

However, the mechanism of procaspase-3 activation cascade induced by D-galactosamine remains unknown (see Section 4).

(2) TUNNEL-staining method, which is the most established DNA nick formation in the nucleus, was examined in these livers. As shown in Fig. 3, the significant nick staining of nuclear DNA was observed in the livers treated with D-galactosamine, while nick formations was significantly suppressed by cotreatment with EGCG. These data show that D-galactosamine induced liver injury resulted in caspase-3 mediated apoptosis and the apoptosis was significantly suppressed by EGCG administration.

(3) Increased activities of AST and ALT in the serum by D-galactosamine administration, which are the established marker for hepatocyte injury, were also completely suppressed by cotreatment with EGCG dose-dependently as shown in Table 2. EGCG showed an effective protecting effect for the liver injury mediated by caspase-3.

4. Discussion

There are several papers on cancer prevention by tea-catechin derivatives, which appear to contradict our own data.

Table 2
Elevation of caspase-3 activities in rat liver cytoplasm in vivo and the activities of AST and ALT in the serum following D-galactosamine administration, and the preventions by EGCG treatment in vivo

	Caspase-3 activities in liver (AFC nM/mg/h)	Aminotransferases in serum (IU/l)	
		AST	ALT
Control LPS	<100	<37.8	<5.8
D-GalN	1000.0	450.0	300.0
D-GalN + LPS	5500.0	5229.3	1438.3
D-GalN + LPS + EGCG 10 mg	3500.0	–	–
D-GalN + LPS + EGCG 30 mg	300.0	320.5	114.0
D-GalN + LPS + EGCG 50 mg	100.0	<100	<100

0.5 g/kg D-galactosamine with 50 μg/kg LPS was administered once intraperitoneally. The D-galactosamine administration method and the preparations of the liver cytoplasm for the caspase-3 assay are described in Section 2.2. The injection doses of EGCG are mg/head. Elevation of caspase-3 activities in the liver cytoplasm in D-galactosamine-induced apoptosis and the preventions by EGCG are in the left columns. The dose-dependent suppressions of caspase-3 activities by EGCG administration are represented in the left columns. All data represent the means ± S.E.M. ($n = 5$) with $^{*}P < 0.01$.

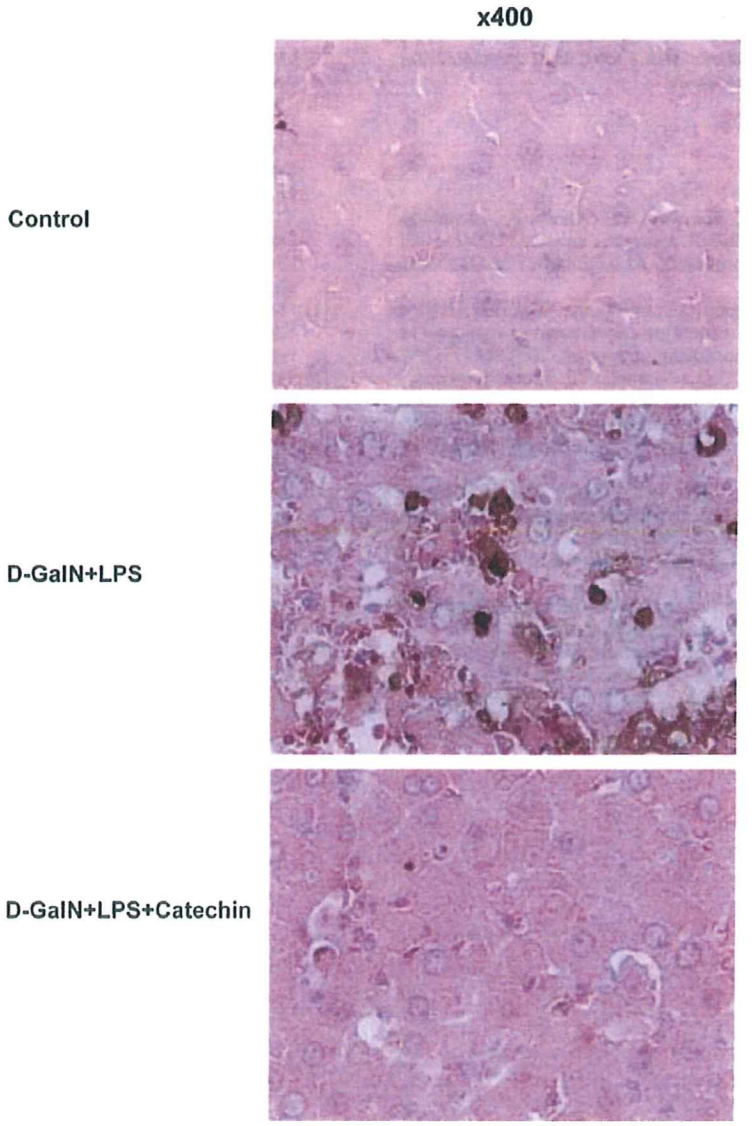

Fig. 3. Hepatocyte apoptosis images using TUNNEL-staining induced by D-galactosamine plus LPS and its prevention by EGCG cotreatment. The staining method is described in Section 2.2. These images are 400× magnification. Top image shows the control liver, the middle image shows liver administrated D-galactosamine plus LPS and the suppression profile by EGCG is shown in the bottom image.

However, this is completely different phenomenon from the following reasons; the reported effective concentration of catechin for cancer prevention is very high 10^{-3}–10^{-4} M [13], these concentrations are not physiological and appear to be toxic concentration. On the other hand, inhibition of caspase-3 by catechins was 10^{-6}–10^{-7} M in vitro and in vivo. Furthermore, these papers do not mention on the relationship between cancer cell death and apoptosis mediated by caspases [13–15]. Some papers reported that catechin stimulates release of TNF-α and enhances effect of anticancer drugs in vivo. While there is data demonstrating the prevention of oncogenesis in vivo, there is no research at the molecular level [14,15].

There are two possible mechanisms by which catechin suppresses hepatocyte apoptosis induced by D-galactosamine administration. One is due to direct inhibition of caspase-3 activity and the other is due to elimination of O_2^-, which is produced by D-galactosamine-protein binding through Maillard reaction. Both mechanisms are likely.

Caspase-3 is constructed from a heterotetramer, which is composed of two pairs of heterodimers. Each unit is composed of a long chain and a short chain. The substrate-binding site is located in the long chains. The interaction between the long chain and short chain and also the unit-to-unit interactions are susceptible to allosteric effectors. For example, it has been reported by Hardy et al. [11] using synthetic allosteric inhibitors that the inhibitor-binding site of the caspase-3 molecule is different from the substrate binding site. They also reported that the –SH of these inhibitors can form a disulfide bond with the cysteine-SH at amino acid 290th of the enzyme, which is different from the active site cysteine in the long chain. The practical conformational change by EGCG will be made clear using X-ray co-crystallography.

Acknowledgments: We thank Dr. Guy Salvesen for his useful advice and Miss Rika Takahashi for her help in preparing the manuscript. This work was supported by Grants-in-Aid from the Japanese Ministry of Education, Sciences and Culture.

References

[1] Enari, M., Sakahira, H., Yokoyama, H., Okawa, K., Iwamatsu, A. and Nagata, S. (1998) A caspase-activated DNase that degrades DNA during apoptosis, and its inhibitor ICAD. Nature 391, 43–50.

[2] Liu, X., Zou, H., Slaughter, C. and Wang, X. (1997) DFF, a heterodimeric protein that functions downstream of caspase-3 to trigger DNA fragmentation during apoptosis. Cell 89, 175–184.

[3] Muntane, J., Montero, J.L., Marchal, T., Perez-Seoane, C., Lozano, J.M., Fraga, E., Pintado, C.O., de la Mata and Mino, G. (1998) Effect of PGE_1 on TNF-α status and hepatic D-galactosamine-induced apoptosis in rats. J. Gastroenterol. Hepatol. 13, 197–207.

[4] Galanos, C., Freudenberg, M.A. and Reutter, W. (1979) Galactosamine-induced sensitization to the lethal effects of endotoxin. Proc. Natl. Acad. Sci. USA 76, 5939–5943.

[5] Korsmeyer, S.J. (1995) Regulators of cell death. Trends Genet. 11, 101–105.

[6] Williams, G.T. and Smith, C.A. (1993) Molecular regulation of apoptosis: genetic controls on cell death. Cell 74, 777–779.

[7] Villa, P., Kaufmann, S.H. and Earnshaw, W.C. (1997) Caspase and caspase inhibitors. Trends Biochem. Sci. 22, 388–393.

[8] Stennicke, H.R., Jurgensmeier, J.M., Shin, H., Deveraux, Q., Wolf, B.B., Yang, X., Zhou, Q., Ellerby, H.M., Ellerby, L.M., Bredesen, D., Green, D.R., Reed, J.C., Froelich, C.J. and Salvesen, G.S. () Pro-caspase-3 is a major physiologic target of caspase-8. J. Biol. Chem. 273, 27084–27090.

[9] Salvesen, G.S. and Dixit, V.M. (1997) Intracellular signaling by proteolysis. Cell 91, 443–446.

[10] Thornberry, N.A., Bull, H.G., Calaycay, J.R., Chapman, K.T., Howard, A.D., Kostura, M.J., Miller, D.K, Molineaux, S.M., Weidner, J.R, Aunins, J., Elliston, K.O., Ayala, J.M., Casano, F.J., Chin, J., Ding, G.J.-F., Egger, L.A., Gaffney, E.P., Limjuco, G., Palyha, O.C., Raju, S.M., Ralond, M., Salley, J.P., Yamin, T.T., Lee, T.D., Shively, J.E., MacCross, M., Mumford, R.A., Schumidt, J.A. and Tocci, M.J. (1992) A novel heterodimeric cysteine protease is required for interleukin-1 beta processing in monocytes. Nature 356, 768–774.

[11] Hardy, J.A., Lam, J., Nguyen, J.T., O'Brien, T. and Wells, J.A. (2004) Discovery of an allosteric site in the caspases. Proc. Natl. Acad. Sci. USA 101, 12461–12466.

[12] Nguyen, J.T. and Wells, J.A. (2003) Direct activation of the apoptosis machinery as a mechanism to target cancer cells. Proc. Natl. Acad. Sci. USA 100, 7533–7538.

[13] Okabe, S., Ochiai, Y., Aida, M., Park, K., Kim, S.J., Nomura, T., Suganuma, M. and Fujiki, H. (1999) Mechanistic aspects of green tea as a cancer preventive: effect of components on human stomach cancer cell lines. Jpn. J. Cancer Res. 90, 733–739.

[14] Suganuma, M., Okabe, S., Kai, Y., Sueoka, N., Sueoka, E. and Fujiki, H. (1999) Synergistic effects of (−)-epigallocatechin gallate with (−)-epicatechin, sulindac, or tamoxifen on cancer-preventive activity in the human lung cancer cell line PC-9. Cancer Res. 59, 44–47.

[15] Suganuma, M., Sueoka, E., Sueoka, N., Okabe, S. and Fujiki, H. (2000) Mechanisms of cancer prevention by tea polyphenols based on inhibition of TNF-alpha expression. Biofactors 13, 67–72.

[16] Fleischer, S. and Kervina, M. (1974) Subcellular fractionation of rat liver. Methods Enzymol. 31, 6–41.

American Journal of Pathology, Vol. 167, No. 4, October 2005

Immunology and Infectious Diseases

Analysis of *in Vivo* Role of α-Fodrin Autoantigen in Primary Sjögren's Syndrome

Katsushi Miyazaki,*† Noriaki Takeda,† Naozumi Ishimaru,* Fumie Omotehara,* Rieko Arakaki,* and Yoshio Hayashi*

From the Department of Pathology, Tokushima University School of Dentistry, Tokushima; and the Department of Otolaryngology,† The University of Tokushima, School of Medicine, Tokushima, Japan*

The α-fodrin N-terminal portion (AFN) autoantigen mediates *in vivo* immunoregulation of autoimmune responses in primary Sjögren's syndrome (SS). We further examined this process and found that cleavage products of AFN were frequently detected in the salivary gland duct cells of SS patients. In *in vitro* studies using human salivary gland HSY cells, anti-Fas-induced apoptosis resulted in specific cleavage of α-fodrin into the 120-kd fragment, in association of α-fodrin with μ-calpain, and activation of caspase 3. Significant proliferative responses against AFN autoantigen were observed in the peripheral blood mononuclear cells (PBMCs) from SS patients with higher pathological score (grade 4) and with short duration from onset (within 5 years). *In vivo* roles of AFN peptides were investigated using PBMCs from patients with SS, systemic lupus erythematosus, and rheumatoid arthritis. Significant proliferative T-cell responses of PBMCs to AFN peptide were detected in SS but not in systemic lupus erythematosus or rheumatoid arthritis. AFN peptide induced Th1-immune responses and accelerated down-regulation of Fas-mediated T-cell apoptosis in SS. Our data further elucidate the *in vivo* role of AFN autoantigen on the development of SS and suggest that the AFN autoantigen is a novel participant in peripheral tolerance. *(Am J Pathol 2005, 167:1051–1059)*

Organ-specific autoimmune diseases are characterized by tissue destruction and functional decline due to autoreactive T cells that escape self-tolerance.[1,2] Primary Sjögren's syndrome (SS) is an autoimmune disorder characterized by lymphocytic infiltrates and destruction of the salivary and lacrimal glands, and systemic production of autoantibodies to the ribonucleoprotein particles SS-A/Ro and SS-B/La.[3–5] SS is a T-cell-mediated autoimmune disease, and autoreactive T cells bearing CD4 molecule may recognize unknown self antigen-triggering autoimmunity in the salivary and lacrimal glands, leading to clinical symptoms of dryness of the mouth and eyes (sicca syndrome).[6,7] Accumulated evidence suggest an important role of apoptosis in disease pathogenesis of SS.[8] Previously we have identified a 120-kd α-fodrin autoantigen in the pathogenesis of primary SS,[9] but the role of autoantigen that render *in vivo* immunoregulation remains unclear.

Although an important role for T cells on the development of organ-specific autoimmune disease has been argued, it is not known whether disease is initiated by a restrained inflammatory reaction to an organ-specific autoantigen. Autoreactive T cells generally respond to a limited number of immunodominant epitopes in self-antigenic proteins including myelin basic protein, thyroglobulin, and glutamic acid decarboxylase.[10–12] α-Fodrin is a ubiquitous, heterodimeric calmodulin-binding protein[13] found to be cleaved by calcium-activated protease (calpain) in apoptotic T cells, and by calpain and caspase family cysteine proteases[14] in anti-Fas-stimulated Jurkat cells and/or neuronal apoptosis.[15–17] Previous reports have demonstrated evidence that caspase 3 is required for α-fodrin cleavage during apoptosis.[18–20] In Jurkat cells, caspase 3-like proteases have been reported to cleave α-fodrin and poly (ADP-ribose) polymerase but with differential sensitivity to the caspase 3 inhibitor, DEVD-fmk.[20] In neuroblastoma cells, treatment with staurosporin induced cleavage of α-fodrin at both caspase 3 and calpain cleavage sites.[21] Therefore, we speculate that an increase in enzymatic activity of apoptotic proteases is involved in the progression of α-fodrin proteolysis during apoptosis of human salivary gland cells. In this study, we analyzed Fas-mediated apoptosis in SS

Supported in part by the Ministry of Education, Science, and Culture of Japan (grants-in-aid for scientific research nos. 12307040 and 12557022).

Accepted for publication July 5, 2005.

Address reprint requests to Yoshio Hayashi, Department of Pathology, Tokushima University School of Dentistry, 3 Kuramotocho, Tokushima 770, Japan. E-mail: hayashi@dent.tokushima-u.ac.jp.

salivary glands, and the *in vivo* role of the autoantigen for T-cell response, cytokine production, and peripheral tolerance.

Materials and Methods

Patients with Autoimmune Diseases

Peripheral blood samples from 18 patients with primary SS, 6 systemic lupus erythematosus (SLE), and 5 rheumatoid arthritis (RA), and from age-matched healthy donors (n = 18) were obtained from the Tokushima University Hospital, Tokushima, Japan. SLE and RA patients were diagnosed based on American College of Rheumatology criteria.[22,23] All patients with SS were female, had documented xerostomia and keratoconjunctivitis sicca, and fulfilled San Diego criteria for the diagnosis of SS.[3] Patients with secondary SS were carefully excluded. All patients with SS had focus scores of greater than 2 in their lip biopsy and all tested positive for autoantibodies against Ro, and 15 of 18 SS patients had autoantibodies against 120-kd α-fodrin by Western blotting. Analysis was performed under the certification of the ethics board of Tokushima University Hospital.

Immunohistology

Immunohistology was performed on freshly frozen sections (4 μm in thickness) by the biotin-avidin immunoperoxidase method using ABC reagent (Vector Laboratories, Burlingame, CA). Briefly, freshly frozen sections were fixed in acetone for 10 minutes, rinsed in phosphate-buffered saline (PBS, pH 7.2), and incubated with an appropriate blocking reagent (Vector Laboratories) for 20 minutes. They were incubated for 1 hour with biotinylated mouse monoclonal antibodies (mAbs) to CD4, CD8, L26(CD20) (BD Bioscience, San Jose, CA), and to Fas and FasL (BD PharMingen, San Diego, CA). To detect the cleavage product of α-fodrin, polyclonal rabbit Abs raised against the synthetic peptide to the purified 120-kd antigen corresponding to the identified 20 amino acid residues (RQKLEDSYRFQFFQRDAEEL) were developed and used.[9] Isotype-matched sera were used as controls, respectively.

Production of Recombinant α-Fodrin

Recombinant α-fodrin N-terminus (AFN) protein (JS-1), the cDNA encoding human α-fodrin (JS-1:1,1784 bp)[9] was constructed by inserting cDNA into the *Eco*RI site of pGEX-2T. Glutathione *S*-transferase fusion protein was expressed and purified using a glutathione *S*-transferase gene fusion system (Amersham Bioscience, Piscataway, NJ).

Synthetic Peptides

AFN peptides identical to JS-1 region were synthesized using tent-butoxycarbonyl chemistry on a model 430A peptide synthesizer (Applied Biosystems, Foster City, CA). A total of 45 synthetic peptides that were designed to be 20-amino acid residues in length, overlapping by five-amino acid residues were generated. As control peptide, laminin fragment peptide 929-933 (Sigma Chemical Co., St. Louis, MO) was used.

Proliferative T-Cell Response

Freshly isolated peripheral blood mononuclear cells (PBMCs) from SS patients and age-matched controls were assayed. When necessary, isolated $CD4^+$ and $CD8^+$ T cells from PBMCs using magnetic beads (Dynal, Oslo, Norway) were assayed. Single cell suspensions were cultured in 96-well flat-bottom microtiter plates (5×10^5 cells/well) in RPMI 1640 containing 10% fetal calf serum, penicillin/streptomycin, and β-mercaptoethanol. Cells were cultured with 10 μg/ml JS-1 protein, 10 μg/ml AFN peptide, and 2.0 μg/ml Con A (EY Laboratories, San Mateo, CA). To confirm the immunoreactivity with the AFN protein (JS-1), 2×10^5 $CD4^+$ and $CD8^+$ T cells from PBMCs of SS patients and controls were co-cultured with irradiated T-cell-depleted PBMCs as antigen-presenting cells, and stimulated with 0 to 20 μg/ml JS-1 for 72 hours. During the last 8 hours of the 72-hour culture period, 1 μCi of [^{3}H]thymidine was added per well, and the incorporated radioactivity was determined using an automated β liquid scintillation counter.

Flow Cytometric Analysis

For analysis of intracellular cytokines, monensin (Wako Pure Chemical, Osaka, Japan) was added at 2 μmol/L to isolated PBMCs (10^6/ml), and 2 hours later the cells were collected, labeled with anti-CD4-PE (BD PharMingen), fixed with 4% paraformaldehyde for 10 minutes at 4°C, and then permeabilized with 0.1% saponin in PBS at room temperature for 10 minutes. Cells were incubated with anti-interleukin (IL)-2-fluorescein isothiocyanate (FITC) (8 μg/ml; BD PharMingen), anti-IL-4-FITC (5 μg/ml; BD PharMingen), and anti-interferon (IFN)-γ-FITC (1 μg/ml; BD PharMingen), respectively, and analyzed on a EPICS flow cytometer (Beckman Coulter, Miami, FL). For analysis of Fas and FasL expression, isolated PBMCs from SS patients when pulsed with AFN peptide (10 μg/ml) were assayed by flow cytometry gated on $CD4^+$ T cells, using anti-Fas and anti-FasL mAb (BD PharMingen). Mean fluorescence intensity was calculated using the fluorescence intensity of staining for mAbs to Fas or FasL and isotype-matched control measured by flow cytometry. Apoptotic cells were detected by flow cytometry with an EPICS (Beckman Coulter) using the Annexin V-FITC apoptosis detection kit (Genzyme, Cambridge, MA).

Cell Culture and Induction of Apoptosis

Human parotid salivary gland HSY cells[24] were grown in Dulbecco's modified Eagle's medium supplemented with 10% heat-inactivated fetal calf serum, 100 U/ml penicillin, and 100 μg/ml streptomycin in a humidified atmosphere

of 5% CO_2 in air at 37°C. The cells were maintained in a logarithmic growth phase by routine passage every 2 to 3 days. Apoptosis was induced in HSY cells by anti-Fas mAb (clone CH-11; Medical and Biological Laboratories. Co., Ltd., Nagoya, Japan).

Western Blot Analysis

For detection of a cleavage product of α-fodrin, Western blot analysis was performed with anti-α-fodrin mAb (Affiniti, Mamhead, UK). To detect the apoptotic proteases *in vitro*, Western blot analysis was performed using mouse mAbs to μ-calpain (clone 9; Chemicon Int., Temecula, CA) specific for catalytic subunit (80 kd), calpastatin (clone 1F7E3D10; Calbiochem, San Diego, CA) specific for amino acids 543 to 673 encoding domain IV (150, 125, 90, and 70 kd), and caspase 3 (3G2; Transduction Laboratories, Lexington, KY) specific for amino acids 28 to 44 encoding large subunit (17/19 kd). The cells were homogenized in 20 mmol/L Tris-HCl buffer (pH 7.4) containing 5 mmol/L ethylene diamine tetraacetic acid, 10 μl/ml protease inhibitor cocktail (Sigma Chemical Co.) and 0.2% Triton X-100. After centrifugation for 20 minutes at 12,000 × *g* at 4°C, supernatant was extracted and used for cytoplasmic protein. Pellets were homogenized in 20 mmol/L Tris-HCl buffer containing 2% Triton X-100. Protein binding was visualized with ECL Western blotting reagent (Amersham Bioscience). Protease inhibitors included leupeptin, E64, pepstatin (Wako Pure Chemicals), calpain inhibitor peptide (Sigma Chemical Co.), and caspase inhibitors [Ac-YVAD-CHO (ICN, Costa Mesa, CA); Z-VAD-fmk (ICN)].

Sequential Activation of Caspase-Like Proteases

The caspase 3-like activity in anti-Fas mAb-treated HSY cell extracts was determined using fluorescent substrate.[25] Cell lysates were diluted with 0.5 ml of standard buffer, and incubated at 30°C for 30 minutes with 1 μmol/L fluorescent substrate. The specific inhibitor for caspase 3 (Z-DEVD-fmk) was added to the reaction mixture at a concentration of 1 μmol/L. Specific caspase 3-like activity was determined by subtracting the values obtained in the presence of inhibitors. The fluorescent substrate, MOCAc-DEVD (dnp)-NH_2 was custom-synthesized at the Peptide Institute (Osaka, Japan). The fluorescence of the cleaved substrates was determined using a spectrofluorometer set at an excitation wavelength of 328 nm and an emission wavelength of 393 nm.

Cell Transfection

cDNAs for full-length caspase 3 and μ-calpain obtained by polymerase chain reaction were subcloned into the pCRII vector (Invitrogen Co., Carlsbad, CA). All constructs were confirmed by DNA sequencing. For expression experiments, DNA fragments were subcloned into pcDNA3.1 expression vector (Invitrogen Co.). HSY cells were transfected with the pcDNA3.1 expression vectors using the Lipofectamine reagent according to the manufacturer's instruction (Invitrogen Co.). The cells were transfected with the individual plasmid DNA and the total amount of DNA transfected was adjusted to 10 μg with pcDNA3.1 for each 100-mm dish or 3 μg for each 60-mm dish. After a 5-hour incubation with the DNA/lipid mixture, the cells were washed with PBS before replenishing with growth media. The cells were harvested 24 hours after transfection and lysed in Tris-HCl buffer.

Results

Involvement of Apoptotic Cascade in SS Salivary Glands

Immunohistochemical analysis revealed that a majority of infiltrating cells were $CD4^+$, and that a small number of $CD8^+$ cells were present in the SS salivary glands. $L26^+$ B cells were sporadically present in the inflammatory lesions (data not shown). Shown in Figure 1, A and B, are photomicrographs taken from representative data. Immunofluorescence analysis revealed that a large number of infiltrating lymphoid cells bear FasL in SS salivary glands (Figure 1C), and epithelial duct cells stained positively with Fas on their cell surface (Figure 1D). Some acinar cells were stained negligibly positive with both anti-FasL and anti-Fas antibodies, but most acinar cells were negative. Immunofluorescence analysis using polyclonal Ab against synthetic 120-kd α-fodrin[9] demonstrated that a cleavage product of α-fodrin was present in epithelial duct cells of the labial salivary gland biopsies from SS patients, but not in control glands (Figure 1, E and F). Western blot analysis confirmed the same results (Figure 1G), indicating that a cleavage product of 120-kd α-fodrin is present in the diseased glands with SS.

In Vitro *Cleavage of α-Fodrin Induced by Apoptotic Stimuli*

We examined the *in vitro* cleavage of α-fodrin using HSY and Jurkat cells induced by anti-Fas mAb (ranging from 1 to 1000 ng/ml^{-1}) apoptotic stimuli. Anti-Fas (CH-11)-stimulated apoptosis in HSY cells was confirmed by flow cytometric analysis using an apoptosis detection kit as well as in Jurkat cells (Figure 2A). Western blot analysis demonstrated that the 240-kd α-fodrin on apoptotic HSY cells was cleaved into smaller 120-kd fragments in dose-dependent manner of anti-Fas mAb (Figure 2B). We next examined whether α-fodrin cleavage into the 120-kd fragment on apoptotic HSY cells could be blocked by preincubation with specific protease inhibitors. In apoptotic HSY cells, a combination of calpain inhibitor peptide and caspase inhibitor (Z-VAD-fmk) entirely blocked the formation of 120-kd α-fodrin, whereas calpain inhibitor peptide alone could not block 120-kd formation (Figure 2C). Caspase inhibitor alone could block considerably 120-kd formation. Cysteine protease inhibitors (E64), serine pro-

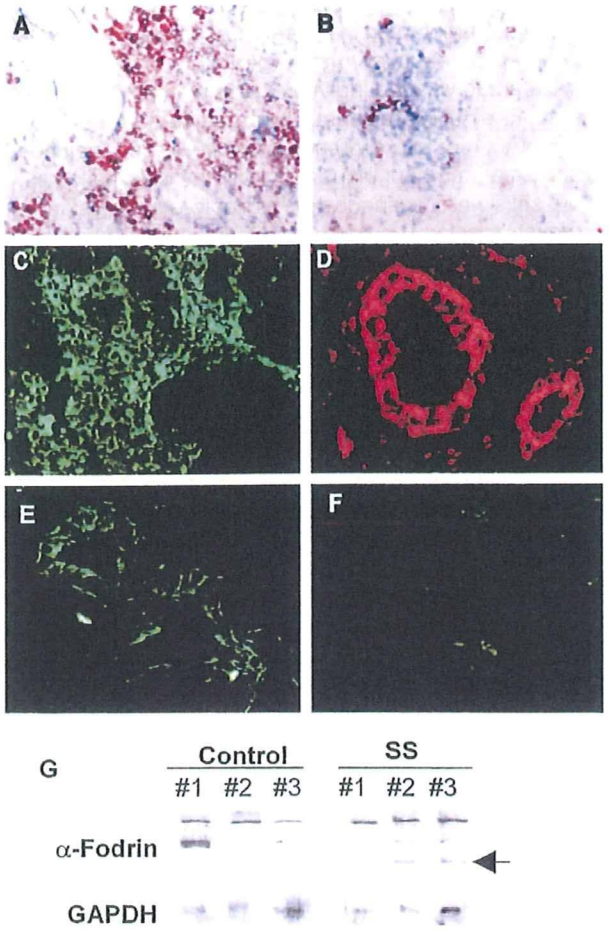

Figure 1. Representative immunohistological features in the labial gland biopsies. A majority of infiltrating cells were $CD4^+$ (**A**), and a small number of $CD8^+$ T cells (**B**) were present in the SS salivary glands. Five samples were examined. Immunofluorescence analysis revealed that the majority of tissue-infiltrating lymphoid cells bear FasL (**C**), and epithelial duct cells stained positively with Fas on their cell surface (**D**) in SS salivary glands. Isotype-matched controls were stained negatively. Six samples for each were examined. A cleavage product of 120-kd α-fodrin was present exclusively in epithelial duct cells of the SS salivary glands (**E**), but not in control salivary glands (**F**). Six samples for each were examined. Detection of a cleavage product of 120-kd α-fodrin in the labial salivary gland biopsies with SS (no. 1, no. 2, and no. 3), but not in control individuals (no. 1, no. 2, and no. 3) on Western blotting (**G**). Eight samples for each were examined.

tease inhibitor (leupeptin), and acidic protease inhibitor (pepstatin) had no effect on 120-kd α-fodrin cleavage.

Calpain and Caspase Mediated α-Fodrin Cleavage

We investigated whether cysteine proteases are involved in α-fodrin cleavage on apoptotic HSY cells. We found a constitutive expression of μ-calpain, and its time-dependent increase in anti-Fas-stimulated HSY cells (Figure 3A). Of note is that abundant calpastatin activity is shown to be constitutively expressed more than calpain expression, and a time-dependent decrease of calpastatin expression was observed in apoptotic HSY cells, not in Jurkat cells (Figure 3A). It can be speculated that μ-calpain activity could be considerably affected by endogenous calpastatin during apoptosis in HSY cells. We confirmed a time-dependent increase in the active form of μ-calpain in apoptotic HSY cells (Figure 3A). Anti-Fas-stimulated HSY cells were positive for mAbs to caspase 3 in association with apoptosis (Figure 3B). Moreover, the caspase 3-like activities in anti-Fas Ab-stimulated HSY cell extracts were determined using fluorescent substrates (Figure 3B).[25] To confirm the role of caspase 3 and μ-calpain proteins in induction of α-fodrin cleavage, full-length caspase 3 and μ-calpain cDNAs were transiently overexpressed in HSY cells, and cleavage product of 120-kd α-fodrin was examined by anti-α-fodrin Ab. Analysis of lysates from caspase 3 and μ-calpain cDNA co-transfected cells with Western blotting revealed a significant increase (approximately fivefold to sevenfold) of 120-kd α-fodrin in the level of expression of caspase 3 or μ-calpain in cells transfected with respective cDNA (Figure 3C).

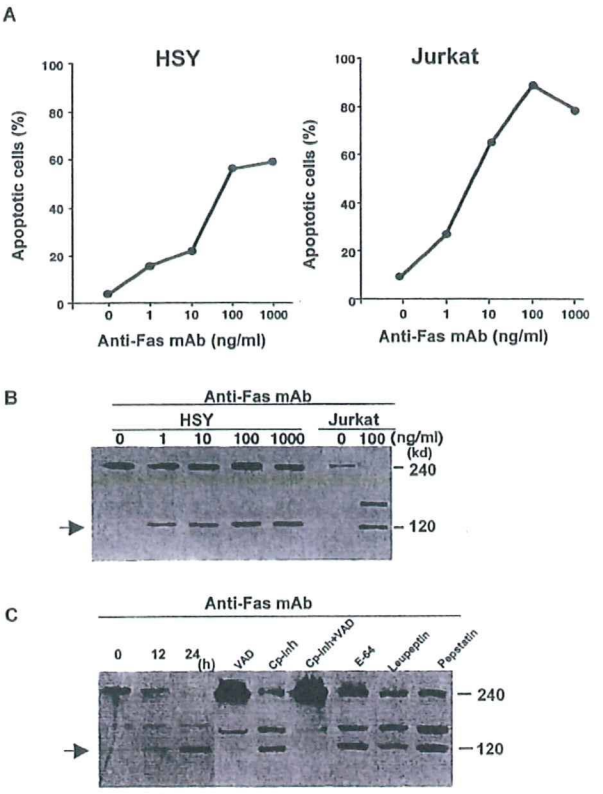

Figure 2. Anti-Fas-induced apoptosis in HSY and Jurkat cells. **A:** The HSY and Jurkat cell apoptosis induced by anti-Fas mAb (CH-11) stimulation was determined by flow cytometry of DNA content of nuclei with PI and annexin V. **B:** Western blot analysis demonstrated 120-kd α-fodrin in apoptotic HSY and Jurkat cells in a dose-dependent manner. **C:** Effects of protease inhibitors on α-fodrin cleavage in apoptotic HSY cells. Proteolytic cleavage of α-fodrin to 120 kd in Fas-stimulated HSY cells is blocked by a combination of a calpain inhibitor peptide and caspase inhibitors (Z-VAD-fmk), but not by E64, leupeptin, and lepstatin. Calpain inhibitor peptide alone could not inhibit the 120-kd α-fodrin formation.

In Vivo *Role of α-Fodrin in SS Patients*

To confirm the immunoreactivity with the AFN protein (JS-1), $CD4^+$ and $CD8^+$ T cells were isolated from PBMCs of SS patients (n = 3) and controls (n = 2), and were co-cultured with irradiated T-cell-depleted

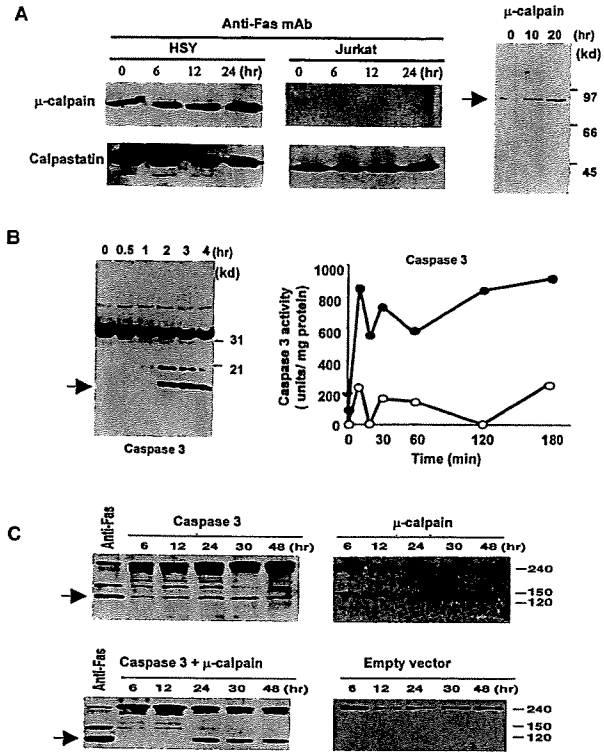

Figure 3. Detection of cysteine proteases in anti-Fas-induced apoptotic HSY cells. Western blot analysis of μ-calpain, and calpastatin in apoptotic HSY and Jurkat cells stimulated with anti-Fas Ab (CH-11). A constitutive expression of μ-calpain, and its time-dependent increase were observed in anti-Fas-stimulated HSY cells. Calpastatin activity is shown to be constitutively expressed more than calpain expression and a time-dependent decrease of calpastatin expression was observed in apoptotic HSY cells, not in Jurkat cells. **A:** Western blot analysis of the active form of μ-calpain in apoptotic HSY cells stimulated with anti-Fas mAb (CH-11). **B:** Western blot analysis showing a time-dependent increase in caspase 3 and sequential activation of caspase 3-like protease in anti-Fas-induced apoptotic HSY cells. The caspase 3-like activity in the lysates (100 mg protein) (**filled circle**) or in the presence of 50 mmol/L MOCAc-DEVD-NH2 (**open circle**) was determined using fluorescent substrates in apoptotic HSY cells. One unit corresponds to the activity that cleaves 1 pmol of the respective fluorescent substrate at 30°C in 30 minutes. **C:** Detection of cleavage product of 120-kd α-fodrin in co-transfected HSY cells overexpressed with full-length caspase 3 and μ-calpain cDNAs. Analysis of lysates from caspase 3 and μ-calpain cDNA co-transfected cells revealed a fivefold to sevenfold increase of 120-kd α-fodrin in the level of expression of caspase 3 or μ-calpain in cells transfected with each construct.

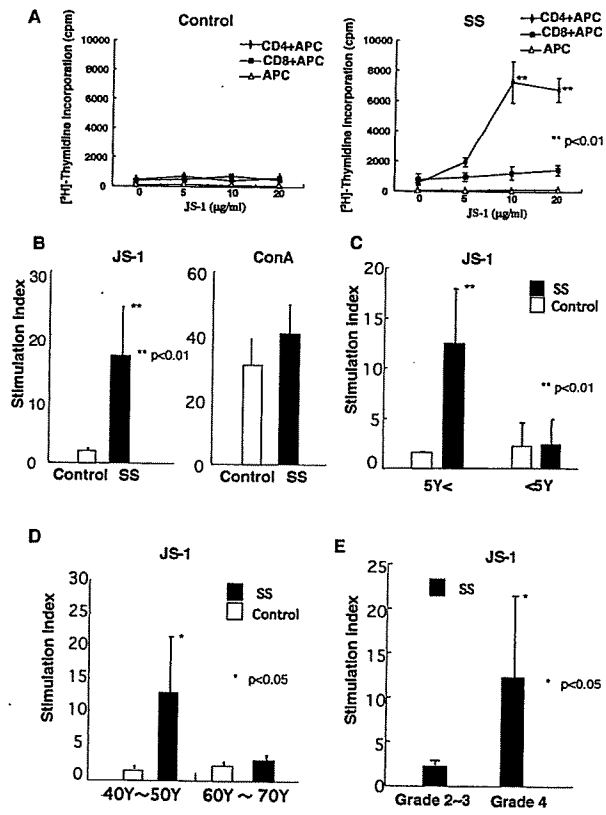

Figure 4. **A:** Significant proliferative $CD4^+$ T-cell responses, not $CD8^+$ T cells, to the AFN protein (JS-1) in the patients with primary SS ($n = 3$), not in age-matched control ($n = 2$) (**$P < 0.01$, Student's *t*-test). **B:** Significant proliferative responses (stimulation indices > 3) of PBMCs to the AFN protein (JS-1) in patients with primary SS ($n = 14$), not in age-matched control ($n = 11$) (**$P < 0.01$, Student's *t*-test). **C:** Proliferative responses to JS-1 of PBMCs from SS patients with short duration (within 5 years) from the onset of the disease ($n = 8$) were significantly higher than those with long duration (more than 5 years) ($n = 6$) (**$P < 0.01$, Student's *t*-test). **D:** Proliferative responses to JS-1 of PBMCs from younger SS patients (40 to 50 years of age) ($n = 8$) were significantly higher than those with older SS patients (60 to 70 years of age) ($n = 6$) (*$P < 0.05$, Student's *t*-test). **E:** Significant proliferative responses to JS-1 protein were observed in PBMCs from SS patients with higher pathological score ($n = 9$, grade 4) than those with lower score ($n = 5$, grade 2 or grade 3) (*$P < 0.05$, Student's *t*-test). All data are expressed as stimulation indices ± SEM.

PBMCs as antigen-presenting cells. Significant proliferative responses were observed in $CD4^+$ T cells from SS patients, not in $CD8^+$ T cells (Figure 4A). Moreover, it has been determined by flow cytometric analysis that the accumulated population in response to both AFN protein (JS-1) and AFN peptide among PBMCs of SS patients is $CD4^+$ T cell (data not shown). Then, we used PBMCs for the proliferation assay. We found proliferative T-cell responses (stimulation indices > 3) to the AFN protein (JS-1) using PBMCs from 14 of 18 patients with SS, not from age-matched healthy patients ($n = 11$) (Figure 4B). Proliferative responses to JS-1 of SS patients with short duration (within 5 years) from the onset of disease ($n = 8$) were significantly higher than those with long duration (longer than 5 years) ($n = 6$) (Figure 4C). Proliferative responses to JS-1 autoantigen with younger SS patients (40 to 50 years of age) ($n = 8$) were significantly higher than those with older SS patients (60 to 70 years of age) ($n = 6$) (Figure 4D). Significant proliferative responses to JS-1 protein were observed in PBMCs from SS patients with higher pathological score ($n = 9$, grade 4) than those with lower score ($n = 5$, grade 2 or grade 3) (Figure 4E). Synthetic peptides of AFN were generated, and immunoregulatory roles were investigated using PBMCs from patients with SS, compared with SLE and RA. Significant proliferative T-cell responses to AFN peptide were detected in PBMCs from 9 of 18 patients with SS, but not with SLE, RA, and healthy controls (Figure 5). We next analyzed intracellular cytokines using isolated PBMCs (10^6/ml). $CD4^+$ T cells from PBMCs with SS patients induce Th1 cytokine (IL-2, IFN-γ) when pulsed with AFN peptide (10 μg/ml) (Figure 6A), not with control laminin fragment peptide (10 μg/ml). We observed a significant decrease in both $CD4^+$ Fas^+ T and $CD4^+$ $FasL^+$ T cells in SS patients,

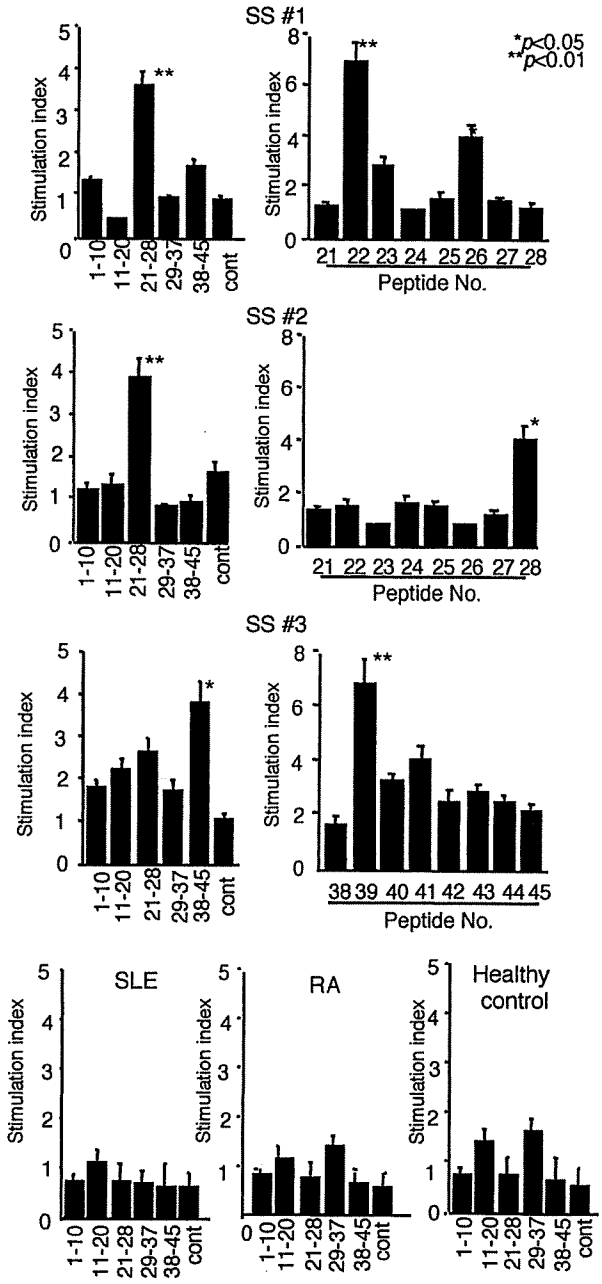

Figure 5. Significant proliferative responses of PBMCs were seen with AFN peptide in the patients with primary SS. Nine of eighteen SS patients examined reacted significantly with single AFN peptide, but not in SLE ($n = 6$), RA ($n = 5$), and age-matched healthy controls ($n = 6$). Representative profiles in three different patients with SS (SS 1, SS 2, SS 3) indicate significant proliferative responses with peptide mixture and individual peptide of p22, p26, p28, and p39 ($^*P < 0.05$, $^{**}P < 0.01$; Student's *t*-test), but not with laminin fragment peptide 929-933 as control antigen. The results are expressed as stimulation indices ± SEM.

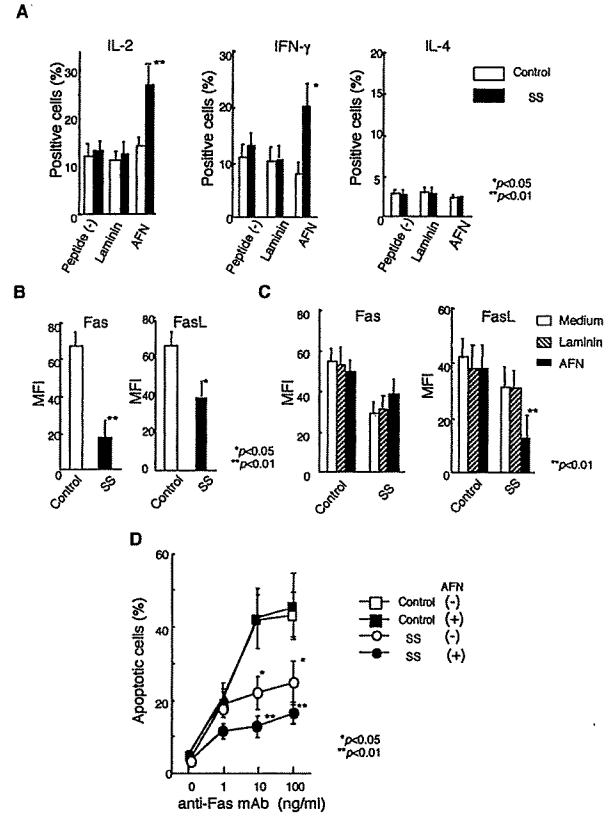

Figure 6. Cytokine profile and Fas-mediated apoptosis in $CD4^+$ T cells from SS patients. **A:** $CD4^+$ T cells from PBMCs with SS patients induce Th1 cytokine (IL-2, IFN-γ), not Th2 cytokine (IL-4) when pulsed with AFN peptide (10 μg/ml) by flow cytometric analysis ($^*P < 0.05$, $^{**}P < 0.01$; Student's *t*-test). Laminin fragment peptide 929-933 (10 μg/ml) was used as control. Five SS patients were analyzed. **B:** Significant decrease in both Fas^+ and $FasL^+$ expression in $CD4^+$ T cells from SS patients, compared with healthy controls ($^*P < 0.05$, $^{**}P < 0.01$; Student's *t*-test). Five SS patients and four healthy controls were analyzed. **C:** AFN peptide-pulsed $CD4^+$ T cells showing significant low intensity of FasL expression, not Fas expression, in SS patients ($^{**}P < 0.01$, Student's *t*-test). MFI (mean fluorescence intensity) indicates the fluorescence intensity of positively stained sample/the fluorescence intensity of its isotype control. Mean fluorescence intensity was calculated using the fluorescence intensity of staining for mAbs to Fas or FasL and isotype-matched control measured by flow cytometry. Five SS patients and four healthy controls were analyzed. **D:** Anti-Fas mAb-stimulated apoptosis showed significant decrease in $CD4^+$ T cells from SS patients than those from healthy control. Moreover, anti-Fas mAb-stimulated apoptosis decreased more significantly in $CD4^+$ T cells from SS patients pulsed with AFN peptide, than those with nonpulsed cells ($^*P < 0.05$, $^{**}P < 0.01$; Student's *t*-test). Five SS patients and four healthy controls were analyzed.

compared with healthy controls (Figure 6B). Moreover, it was demonstrated that AFN peptide-pulsed $CD4^+$ T cells showed a significant low intensity of FasL expression, not Fas expression (Figure 6C). Anti-Fas mAb-stimulated apoptosis showed a significant decrease in $CD4^+$ T cells from SS patients than those from healthy control (Figure 6D). When pulsed with AFN peptide, anti-Fas mAb-stimulated apoptosis decreased more significantly in $CD4^+$ T cells from SS patients.

Discussion

Cleavage of certain autoantigens during apoptosis may reveal immunocryptic epitopes that could potentially induce autoimmune responses in systemic autoimmune diseases.[26,27] We reported previously that a cleavage product of 120-kd α-fodrin may be an important autoantigen on the development of primary SS, and anti-120-kd α-fodrin antibodies have been frequently detected in sera from patients.[9] Although several candidate autoantigens besides α-fodrin have